The glacial history of the southern Svartenhuk Halvø, West Greenland

Lane, T.P., Roberts, D.H., Ó Cofaigh, C., Vieli, A., Moreton, S.

Timothy P. Lane[a], David H. Roberts[b], Colm Ó Cofaigh[b], Andreas Vieli[c], and Steve Moreton[d]

[a] School of Natural Sciences and Psychology, Liverpool John Moores University, Liverpool, L3 3AF, United Kingdom

[b] Department of Geography, South Road, Durham University, UK

[c] Department of Geography, University of Zurich – Irchel, Winterthurerstr. 190, CH-8057 Zurich, Switzerland

[d] NERC Radiocarbon Laboratory, Scottish Enterprise Technology Park, East Kilbride, G75 0QF, United Kingdom

Corresponding author: Timothy P. Lane [t.p.lane@ljmu.ac.uk; 00447817344057]

Abstract

This paper presents a new, detailed geomorphological and sedimentological appraisal of the southern Svartenhuk Halvø in West Greenland. Svartenhuk Halvø is a large, low-altitude landmass which is found in the north-western part of the Uummannaq region. Previous research on the glacial history of this peninsula is limited, but studies have suggested it remained as an ice-free enclave during the Last Glacial Maximum. Previous work has provided biostratigraphic, chronological, and sedimentological evidence for the 'Svartenhuk Marine Event', a period of deposition into a higher than present relative sea-level during an interglacial. It has been dated to MIS 5 and correlated to other interglacial deposits in West Greenland. New geomorphological and sedimentological investigations from this study present a compelling argument for the glaciation of southern Svartenhuk Halvø by valley glaciers and mountain ice caps, suggesting that the existence of this peninsula as an ice free enclave as a misnomer. Ice directional indicators and clast lithological results suggest ice covering Svartenhuk Halvø was sourced from the higher altitude interior of the peninsula and expanded to the present coastline. In a number of valleys, sedimentological evidence points to at least two glacial advances. New shell radiocarbon dates provide 49.8 cal. kyr BP as a maximum age for glaciation, tentatively suggesting glacial advances occurred during the last glacial cycle. Sedimentological evidence of a retreating ice margin is predominately of raised marine origin, and is therefore likely to have occurred during the early phases of a deglaciation, in association with a glacio-isostatically higher sea-level.

1. Introduction

Ice sheets are well known to exert major impacts upon landscape evolution at local, regional and continental scales, and have done throughout the Quaternary (Sugden, 1974; Whillans, 1978). The ice-free periphery of the Greenland Ice Sheet (GrIS) is a unique region in which to investigate landscape evolution, as its form is a result of repeated ice sheet erosion during Pleistocene cold periods and potential interglacial sediment deposition during warm periods. The present ice free landscape of Greenland is dominated by landscapes resulting from ice sheet activity (e.g. areal scour and selective linear erosion), and those formed through the action of independent valley and mountain glacier systems (Lane et al., 2015; Sugden, 1974). During full glacial conditions, the majority of land surrounding Greenland was inundated and covered by thick, ice stream and inter-stream ice as it moved offshore (Funder et al., 2011). At the Last Glacial Maximum (LGM), the GrIS in West Greenland was drained by a series of large, cross-shelf ice streams which terminated at, or close to, the shelf-edge, and produced large trough mouth fans (Lane et al., 2014; Ó Cofaigh et al., 2013a; 2013b; Roberts et al., 2010; 2013). The location and longevity of these systems is likely to have had an important impact upon landscape evolution and modification (Roberts et al., 2010; Roberts et al., 2009; Swift et al., 2008) around the GrIS, and would have been a factor in determining the position of these areas of limited glaciation.

Despite evidence for extensive glacial erosion of the ice free coastal hinterland of Greenland, a number of lowland regions were thought to have remained ice free throughout glacial cycles, acting as refugia for plants during glacial periods (Gelting, 1934), displaying 'little or no evidence of glacial erosion' (Sugden, 1974). Restricted GrIS coverage during the Eemian (MIS 5e) (Dahl-Jensen et al., 2013) and higher than present sea-levels would have made these regions potential sinks for sediments during MIS5e or earlier interglacial periods (Funder et al., 1991; Kelly, 1986). Following this, the absence of erosion by the GrIS has allowed for the preservation of sediments deposited prior to the last glacial cycle. It is possible that the intense focusing of ice flow which occurs in ice streams could have starved peripheral inter-stream areas of warm-based ice, leaving them stranded as fields of cold-based ice (Kleman and Glasser, 2007; Lane et al., 2015). This produces regions exhibiting very restricted evidence for glacial activity proximal to the ice sheet, although it is probable that higher altitude terrain contained small warm-based valley glaciers, cold-based plateau ice-fields, or inter-stream areas (Håkansson et al., 2009). Areas classified as such appear highly localised in their distribution, and it was suggested that a local combination of factors are required to generate and then preserve these landscapes (Sugden, 1974). One such topographic and glaciological setting, identified by Sugden (1974), is the Svartenhuk Halvø. This landmass is thought to have been minimally effected by the nearby Uummannaq Ice Stream (UIS) during glacial periods (Lane et al., 2014; Roberts et al., 2013), instead being occupied by local mountain and plateau glaciers of limited extent. This is thought to have allowed the preservation of extensive deposits, an unusual situation in West Greenland, which is typified by glacially scoured surfaces and an absence of sediments. The deposits on Svartenhuk Halvø are thought to have been deposited during the last interglacial, during a period termed the 'Svartenhuk Marine Event' (SME) (see below for a full explanation of these deposits).

2. Study site

The Uummannaq region covers an area of ~25,000 km^2 (70.33°N to 72.00°N, 50.00°W to 55.00°W) (Figure 1), and is one of the most mountainous areas of West Greenland, with summits reaching >2000 m a.s.l. It is bounded to the north and south by large peninsulas which form large topographic barriers, confining the flux of ice and water from the Uummannaq region to the narrow passages north and south of Ubekendt Ejland. The Svartenhuk Halvø (~ 4,000 km^2) borders the northern edge of the Uummannaq region. The west of the peninsula is formed of transitional basalts and theoliites, the northern central region is formed of hyaloclastite, and the east is picrite and olivine basalt (Figure 2a) (Henderson and Pulvertaft, 1987a; Henderson and Pulvertaft, 1987b). It is an area relatively low in altitude; summit heights in the west of the peninsula are below 1000 m a.s.l., increasing to 1100 – 1200 m a.s.l. in the east. Several small (< 5 km^2) mountain valley glaciers exist in the central and west portions of the peninsula (Figure 2b). The southern coast is characterised by four large valley systems which drain the interior of the peninsula. At the LGM, areas to the east and south of Svartenhuk Halvø were occupied by the UIS, with LGM ice surface elevation constrained to ~ 1400 m a.s.l. (Lane et al., 2014; Ó Cofaigh et al., 2013b; Roberts et al., 2013). Trunk flow from the northern UIS would have been deflected south by Ubekendt Ejland into Igdlorssuit Sund, coalescing with southern outlet glaciers (Figure 1) (Dowdeswell et al., 2014; Lane et al., 2014; Ó Cofaigh et al., 2013b; Roberts et al., 2013).

3. Previous study

3.1. Geomorphology and sedimentology

The Svartenhuk Halvø region has been subject to a long history of sedimentological and palaeoecological investigation (Tables 1 and 2) (Bennike et al., 1994; Funder, 1989; Laursen, 1944; Rink, 1853; Steenstrup, 1883). Early research reported the area to be dominated by a fluvial system with a widespread, thin sediment cover (Figure 2b) (Laursen, 1944). Clasts from fluvial, deltaic, and beach settings are almost exclusively derived from local basaltic material (Laursen, 1944). A number of the mountain valley glaciers in the interior of the peninsula contain moraines indicating periods of more spatially extensive ice cover (Laursen, 1944). From aerial photo mapping and field analysis Sugden (1974) classified southern and western Svartenhuk Halvø as displaying little or no glacial erosion, with the north and east classified as landscapes of cirque glaciers and plateau remnants. Recent mapping has reclassified a larger proportion of the peninsula as areas of mountain valley and cirque glaciers (Lane et al., 2015). Initial sedimentological studies in Svartenhuk Halvø reported the presence of deltaic deposits with in-situ marine molluscs thought to relate to glacioisostatically uplifted sediments (Funder, 1989). A thin cover of morainic material, containing occasional erratic boulders, is recorded from the interior of the peninsula (Laursen, 1944). The southern and western coastlines contain widespread shell-bearing littoral gravel and sub-littoral muds, with a single exposure of diamicton (Bennike et al., 1994). These sites are thought to represent palaeo- spits, cuspate forelands, alluvial cones, and deltas, which extend up to 35 m a.s.l. (Bennike et

al., 1994), with possible evidence for later, localised Late Weichselian glaciation. Biostratigraphic investigation of the sediments demonstrated some discrepancy between the mollusc data and the microfossil data (Bennike et al., 1994).

3.2. Chronology

The majority of radiocarbon dates from shells across Svartenhuk Halvø returned non-finite ages of >40,000 ^{14}C yrs BP, with one finite age of 37,970 +2470/-1890 ^{14}C yrs BP (Bennike et al., 1994; Kelly, 1986). These age determinations are from single shells at each site, thus with no within-site reproducibility at present. Amino acid determinations from marine shells taken from sites throughout Svartenhuk Halvø returned aIle/Ile ratios of F = 0.182 and T = 0.0236 (12 samples) (Kelly, 1986), and F = 0.173 and T = 0.032 (8 samples) (Bennike et al., 1994), suggesting an age of >55 kyr (Kelly, 1986). More recent work on amino acid ratios and their use as a chronometer has been undertaken in West Greenland (Briner et al., 2014), but this recent work has not been undertaken on Svartenhuk Halvø. Finally, two U/Th dates from marine shells returned ages of >89 kyr and 115 kyr (no errors given) (quoted in Funder et al., 1994; as from Kelly, 1986). On the basis of this chronology, sediments, and macrofossil assemblages found across the Svartenhuk Halvø coastal zone were proposed to represent a period of elevated sea-level (~35 m a.s.l.) in MIS 5e-a, ~115 kyr, named the SME (Bennike et al., 1994; Funder et al., 1991; Kelly, 1986), correlated with the Thule aminozone in north-west Greenland. The age and preservation of SME sediments supports the hypothesis that ice from the GrIS had minimal impact upon Svartenhuk Halvø during the LGM.

Despite these investigations and interpretations, understanding of Svartenhuk Halvø's late-Quaternary history is poor. The geomorphology of the Svartenhuk Halvø has not been assessed in detail, meaning that a comprehensive understanding of the depositional environments of the Svartenhuk Halvø sediments is lacking. Moreover, the palaeo-environmental reconstructions from biostratigraphy are conflicting. Biostratigraphic indicators from 12 sites have provided marine macrofauna reconstructions suggesting conditions analogous the Holocene in North Greenland; ostracod assemblages representing a quiet shallow marine environment analogous to present day Disko Bugt; and foraminiferal assemblages suggesting sub-arctic, glacier distal conditions (Bennike et al., 1994; Kelly, 1986; Laursen, 1944). Furthermore the current chronological framework is based on relatively few dates which are sparsely distributed across region. This paper aims to: (i) reconstruct the pre-LGM and LGM glacial history of the Svartenhuk Halvø landscape; (ii) investigate the morphology and sedimentology of landforms throughout southern coastal Svartenhuk Halvø; (iii) improve the chronological framework for the landforms and deposits in this region, in order to reconstruct the glacial history of the peninsula.

4. Methods

4.1. Geomorphological mapping

Regional geomorphological mapping was carried out using 1:50,000 topographic maps, geological maps (Henderson and Pulvertaft, 1987a; Henderson and Pulvertaft, 1987b), 1:150,000 aerial photographs (Kort and Matrikelstyrelsen) and ASTER GDEMs, focusing upon the southern coast of Svartenhuk Halvø. These were ground truthed in the field. Glacial, glaciofluvial, and fluvial landforms were identified and mapped, and a Garmin GPS 60 used to record their location.

4.2. Sedimentology

Sediment exposures were logged and sketched, noting any lateral sediment variability and macroscale sediment structure. Sediment description adopted a lithofacies approach (Edwards, 1986; Evans and Benn, 2004) and included description of: grain size; depositional and deformation structures; thickness; geometry; colour; clast size; sediment texture; and contacts between lithofacies (Evans and Benn, 2004). Clast form analysis was performed upon clasts from gravel and diamicton units (n=50 per unit), measuring clast morphology and roundness on the Powers' roundness scale (Benn and Ballantyne, 1994). Clast form was presented using ternary diagrams (Benn, 1994; Benn and Ballantyne, 1994; Lukas et al., 2013; Sneed and Folk, 1958). Ternary diagrams use c:a and b:a axis ratios to distinguish equant/blocky ($a \approx b \approx c$), elongate ($a >> b \approx c$), and oblate/platy ($a \approx b > c$) shaped clasts. Clast C40 index (percentage of clasts with a c:a ratio of ≤ 0.4) was used to distinguish blocky from elongate clasts (Ballantyne, 1982; Benn, 1994; Benn and Ballantyne, 1994). RA indexes were calculated by adding the percentages of very angular and angular clasts. Clast fabric data were collected from units of diamicton (Evans and Benn, 2004). The orientation and dip of fifty elongate clasts within a 1 m^2 exposure was measured for each sample. Eigenvalues were calculated for samples, and results were plotted as stereonets and rose diagrams using the RockWare RockWorks software package. Sediment samples were taken from each sedimentary unit for laboratory particle size measurement. Laboratory based particle size was determined for the <2mm fraction using laser diffraction, widely regarded as providing the greatest reproducibility (Goossens, 2008; Sperazza et al., 2004).

4.3. Radiocarbon dating

Shells were collected for radiocarbon dating from sediments at all sites, where found. Where visible, shells were picked from sediment exposures with care using a trowel. In order to ensure that dated shells were *in situ* only paired, articulated bivalves were sampled. Shells were lightly cleaned to remove surficial dirt and then processed at the NERC Radiocarbon Facility, East Kilbride. Here, samples were cleaned in an ultrasonic bath in deionised H_2O for two minutes and then rinsed in deionised H_2O. Once cleaned the outer 20% by weight of shell was removed by controlled hydrolysis with dilute HCl. The samples were then rinsed in deionised water, dried and homogenised. A known weight of the pre-treated sample was hydrolysed to CO2 using 85% orthophosphoric acid at room temperature. The CO2 was converted to graphite by Fe/Zn reduction. Results in this study have

been corrected to $\delta^{13}C_{VPDB}$‰ -25 using the $\delta^{13}C$ values provided in the report. The $\delta^{13}C$ values were measured on a dual inlet stable isotope mass spectrometer (Thermo Scientific Delta V Plus) and are representative of $\delta^{13}C$ in the original, pre-treated sample material.

5. Results

Geomorphological and sedimentological investigations were undertaken in: Arfertuarssuk; Kugssineq and Tasiussaq; and Ulissat (see Figure 2 and Table 1). Logs were taken from each of the valleys, and the sedimentary sequences recorded through these have been sub-divided into five lithofacies associations (see Table 3 for a summary of the lithofacies associations recorded). Geomorphological results are presented by each of these three areas, and sedimentological results and interpretations are presented by lithofacies association.

5.1. Geomorphology

5.1.1. Arfertuarssuk and Quassugaarsuit (Logs 1 - 4)

Arfertuarssuk is a sheltered, northwest to southeast trending, steep-sided fjord in western Svartenhuk Halvø (Figures 2 and 3) bounded by higher altitude terrain (>600 m a.s.l.) to the east and west. The fjord head region and the hinterland to the north rises gently, reaching up to 300 m a.s.l. in altitude. A series of discontinuous erosional benches are incised into the fjord walls up to a height of 68 m a.s.l. These vary in their size and preservation with individual sections reaching up to 500 m in length, and tread depths up to 11 m. In places their surfaces displayed a gravel cap (> 30 cm), formed of coarse gravels held in a sandy matrix. The most prominent bench is at 32 m a.s.l., and backed by a distinct, frost shattered, fossil cliff line. To the southeast it grades into a flat topped alluvial fan (32 m a.s.l.), at the base of a contemporary fluvial channel (Figure 4a).

Alluvial fans (cf. Bull, 1977) are found throughout Arfertuarssuk, formed on terrain to the east, west and north of the fjord. Their surfaces are smooth, displaying gentle apex to toe slopes. Although raised above present sea-level (12 – 32 m a.s.l.) all fans are found at the bases of palaeo-fluvial sources (Figure 3) and are interpreted as coastal alluvial fans which formed through sediment aggradation to sea-level, subsequently raised by glacioisostatic rebound. The largest of these fans in Arfertuarssuk is on the western side of the fjord, emanating from a deeply incised fluvial channel sourced from high altitude terrain to the west (Figures 3 and 4b). The fan extends ~500 m up valley and its surface is graded to ~32-20 m a.s.l. (apex to toe). The fan surface is composed of angular to sub-rounded local basaltic material held within a silty matrix, and has experienced extensive frost heaving.

These are spatially extensive features with flat-topped upper surfaces graded to 12 - 16 m a.s.l. were found at the fjord head (Logs 1-3) and in the mid-fjord (Log 4) of Arfertuarssuk, with no clear source channel. Based upon their geomorphology and sedimentology these are interpreted as raised deltas. At the head of the valley,

a delta appears to infill the southern Quassugaarsuit valley down to the present coastline. Log 4 is taken from a delta on the eastern side of Arfertuarssuk, mid-way up the fjord (Figure 3) and has a flat top with a gentle south-west dip, graded to 16-14 m a.s.l. An exposure of heavily striated *in-situ* bedrock (mean direction 160° - 340°) was found at the base of the delta section (see Figure 3). The narrow, low lying "Unnamed Valley" to the northeast of Logs 1-3 (Figure 3) contains a thick sediment infill which continues inland from the coast for ~800 m. It has a smooth surface which dips downstream towards Arfertuarssuk, at a height of 32 to 16 m a.s.l. The surface has been heavily dissected by contemporary fluvial channels, and grades directly into the upper surfaces of deltas at Logs 1 and 2. Although the surface was generally smooth, a series of circular depressions, up to 4 m in depth and 10 m in diameter were found formed across its surface, with no obvious pattern of distribution. Based upon the morphology of this area it is interpreted as a region of kettled outwash, with an extensive outwash surface cratered by circular kettle holes (Benn and Evans, 2010; Maizels, 1977), resulting from the melt out of blocks detached from the snout of a glacier (Gustavson and Boothroyd, 1987; Price, 1970; Rich, 1943), or through the melt of icebergs deposited on the outwash surface through a flood event (Maizels, 1992). An 80 m long, 1 m high ridge formed of coarse, unsorted sand and gravel, with locally sourced basaltic pebbles and cobbles was found grading into the flat-topped surface from the north. Based upon the form, valley position, and internal sedimentology of the ridge, it is interpreted as a small esker, formed of glaciofluvial sand and gravel (Benn and Evans, 2010; Warren and Ashley, 1994).

Terrain north of Arfertuarssuk is rolling and hilly, and is dominated by the low-lying Quassugaarsuit valley (Figures 3, 4d, 5a, and 5b). The area is characterised by a series of NNW – SSE trending bedrock-controlled ridges, elevated up to 100 m above the surrounding terrain. The summit surfaces of these ridges display either exposed heavily weathered bedrock with weathering pits up to 10 cm deep and frequent tors and micro-tors, or a thin cover of weathered regolith, generally angular autochonous blockfield with some abraded, sub-rounded erratic clasts. Where present, the regolith has been subjected to extended periods of periglacial processes including frost shattering and stone sorting (Figure 5b). Very occasionally weathered bedrock surfaces display fragments of glacial polish and striated faces. Infrequent sub-rounded boulders of local basaltic and far-travelled gneissic lithologies are present up to 400 m a.s.l., perched upon the present land surface. Above this elevation sub-rounded boulders become far less common. A number of the NNW – SSE bedrock ridges within the Quassugaarsuit valley are incised deeply by meltwater channels. The channels are short but deep features (up to 10 m), and appear to cut across local watersheds, forming at ridge interfluves, with no clear meltwater source area. Low lying regions between the bedrock ridges contain well-developed fluvial systems, draining either north-northwest or south-southeast. Clasts within these channels are dominated by local basaltic lithologies, although infrequent gneissic erratics were found, increasing in abundance to the north east of the valley.

A small lobate ridge was mapped on the east of Quassugaarsuit, close to the mouth of the Akulerqut Valley. It is ~2-3 m high, 5 m wide, and only present on the southern side of the valley. Based upon its morphology and position upon the flank of the valley, the ridge is interpreted as a partial remnant of a lateral moraine. A small (0.5 – 1 m high), discontinuous ridge was mapped 500 m up-valley of the moraine, close to the present fluvial channel. It was formed of sub-rounded cobble-sized, locally derived basaltic clasts. On the basis of its mid-valley position, internal sediments, and morphology, this is interpreted as an esker, as defined above (Benn and Evans, 2010; Warren and Ashley, 1994). This valley is sourced from the interior of Svartenhuk Halvø and currently hosts a number of small, independent valley glaciers in its upper reaches.

5.1.2. Kugssineq and Tasiussaq (Logs 5 - 9)

East of Arfertuarssuk, the south coast of Svartenhuk Halvø contains five north-south trending valleys, sourced in the high-level (>1000 m a.s.l.) interior of Svartenhuk Halvø. These valleys are fed by a number of individual, small (<3 km^2) valley glaciers, and have large, U-shaped cross-profiles up to 5km in width. Valley floors are characterised by contemporary tidal flats, salt marshes, and misfit fluvial streams. All valley systems were seen to contain thick sequences of sediment close to the valley mouths, extending up to 3 km inland (Henderson and Pulvertaft, 1987b). These sediments are found deposited in flat-topped fans and deltas, graded to heights of between 14 and 43 m a.s.l., and are bisected by contemporary misfit fluvial systems.

The two most westerly of these valleys are Kugssineq and Tasiussaq (Figures 2 and 6). The Kugssineq valley is a 0.8 km wide, flat-bottomed valley containing a contemporary salt-marsh system. A series of sediments were preserved at the mouth of the valley in a large, flat-topped delta, reaching 18 m a.s.l. The floor of the Tasiussaq valley is characterised by contemporary salt marsh, with a number of large circular pools (Figure 7c). These features were not studied in detail in the field, but their extensive occurrence on the valley floor, and difference in appearance to other valley floors makes them of note. Their circular morphology and the presence of other glacial features in the valley suggests they are submerged kettle holes, and the valley floor represents a kettled sandur (Maizels, 1977). Two discontinuous ridges were mapped on the south side of the valley, between Tasiussaq and Igdlerussat qáqâ valleys (Figure 7b), running sub-parallel to Tasiussaq valley long axis (NE-SW) (Figures 7b and 7c). They are wide and low in relief (<10 m wide, <4 m high) and formed of angular to sub-rounded clasts between pebble and boulder size, and are interpreted as inset lateral moraines (Benn and Evans, 2010; Boulton and Eyles, 1979), relating to the presence of ice within the Tasiussaq valley. High-level terrain outside of these moraines is characterised by frost shattered bedrock, with a thin, patchy cover of weathered regolith. Where bedrock remains intact and exposed, outcrops displayed weathering pits up to 6 cm deep and occasional abraded and striated surfaces (orientation 173-353°). Only basaltic erratics were found on this high-level terrain. The mapped extent of this weathered surface is shown in Figure 6, although based upon field observations it is likely that this type of surface covers the majority of high-altitude areas (>500 m a.s.l.). Terrain

inside of the lateral moraine complex is dominated by fluvial and salt marsh environments. Bedrock surfaces appear less weathered than terrain outside of the moraines, with weathering pits commonly 1-2 cm in depth. Sediments at the mouth of Tasiussaq valley (Figure 7c) are best preserved on the southern side of the valley, close to the neighbouring Igdlerussat qáqâ, in a flat topped delta sequence graded to 16 m a.s.l. (Figure 6 and 7c). A series of low relief, sinuous, ridges were found deposited upon these flat topped deposits, orientated sub-parallel to the Tasiussaq valley and lateral moraines found on higher ground to the south (Figure 7b), interpreted as eskers (Benn and Evans, 2010; Warren and Ashley, 1994). A large sedimentary mound was found in south-west Tasiussaq, south-west of the delta (Log 9), measuring 120 m long by 20 m high. The feature lies below a small valley sourced from high ground to the southeast, close to Igdlerussat qáqâ. The feature appears to have been glacially streamlined, its internal sedimentary structure showing clear evidence of erosion following deposition.

5.1.3. Ulissat (Log 10)

Ulissat is the easternmost of the Svartenhuk Halvø valleys (Figure 2). Extensive sediments are preserved close to the valley mouth and further up-valley in a series of inset deltas and alluvial fans, graded to between 20 and 75 m a.s.l. The highest altitude feature in the valley at 75 m a.s.l. appears as an alluvial fan, emanating from a small (0.25 km^2) bench incised into the bedrock valley wall, backed by a small bedrock incised cliff. This is the highest evidence for marine activity throughout the Svartenhuk Halvø area, and represents the marine limit. A large delta complex is found close to the mouth of the valley, dissected by post-depositional fluvial and coastal erosion, with a series of sub-angular to sub-rounded erratic quartzite boulders resting upon its surface (Figure 9). This delta is flat-topped, with a gentle surface slope, and steeply dipping up-valley face (Figure 9). The surface of the delta reaches 36 m a.s.l. at its highest point, dropping to ~24 m a.s.l. at its down-valley edge. A section was logged from the large delta at the mouth of the valley (Log 10). Tributary fluvial channels up-valley feed into a series of alluvial fans. Kame terraces, poorly formed discontinuous lateral moraines, and a drift limit are found on valley walls.

5.2. Sediment descriptions

As a lithofacies approach was adopted for sediment description and interpretation (Edwards, 1986; Evans and Benn, 2004) the sediments from southern Svartenhuk Halvø have been sub-divided into five distinct lithofacies associations (Table 3). Several of these lithofacies associations were further sub-divided in order to fully characterise the sediment. Clast fabric data are shown in Figures 10 and 11, and sedimentary logs are shown in Figures 12, 13, and 14.

5.2.1. LFA1

LFA1 is a diamicton containing angular to very angular, locally-derived basaltic clasts held within a clay to silty sand matrix. The diamicton appeared in bands of altering colour, varying between layers of red, brown, yellow, and purple. Clast density throughout this lithofacies is variable and in places the diamict is clast-supported. The majority of clasts show a high degree of weathering and extensive brecciation. LFA1 was seen to be transitional into, or interstratified with, *in-situ* bedrock breccias, evidenced by a higher clast density, in places displaying primary bedrock structure (Figure 15). The *in-situ* bedrock appears to have been displaced or thrusted, with the coarse, angular, diamict found between areas of heavily brecciated bedrock.

5.2.2. LFA2

LFA2 is a grey, poor to well-consolidated, generally structureless, matrix-supported diamicton with occasional discontinuous lenses of well-sorted sandy silt (~10 cm thick, ~30 cm wide). Some very crude stratification was visible in section (e.g. facies 5c). Clast abundance is highly variable although the diamict remained matrix supported throughout. The matrix is composed of silt to silty-sand, with particle size peaks at 1000 µm, 150 µm, and 60 µm. It contains abundant marine shell fragments, dominated by *Hiatella arctica* and occasional single valves, although very rare paired valves were found. Clasts are up to 50 cm in diameter, angular to sub-rounded, often striated, and dominated by local basaltic lithologies and occasional gneissic erratics. Clast form data reveal a preference toward blocky to elongate clasts, with C40 values between 38 and 44%, and RA values of 37-42. Clast macro fabrics display NW-SE orientated a-axes, with a subsidiary perpendicular, NE-SW component (Figure 10). S1 values are 0.54, suggesting moderate a-axis clustering, and fabric shapes plot as girdles to moderate clusters (Figures 10 and 11). Striae were measured on boulders found lodged within LFA2, ~100 m to the southwest of Log 1. Results showed highly uniform intra-boulder striae, but high inter-boulder variability, suggesting some boulder rotation subsequent to striation, and during diamicton emplacement (Figure 12). A paired valve from the sediment returned a radiocarbon age of 47.7 cal. kyr BP (Table 4), although it is possible that this is non-finite given it is close to the limit of the technique.

5.2.3. LFA3

LF3a is planar bedded, interstratified silty-clay, silt, and medium sand (Figure 16), with a fine gravel content (average grain size 300 µm). Planar stratification was horizontal, except for Log 9b, where bedding dips west at 2°. Clast supported gravel horizons up to 60 cm thick were found, held within a medium sand. LF3a shows evidence of variable grading, displaying normal grading (e.g. Log 7), inverse grading (e.g. Log 9), and no grading (e.g. Log 8). In places finer beds display distinct evidence of post-depositional loading deformation including convolutions, flames, and pipes. The silty-clay and silt beds contain ubiquitous detrital plant remains, and abundant marine shell fragments and rare whole marine valves were retrieved from fine layers. In Log 9 the abundance of macroscopic plant remains increases dramatically between towards the top of LF3a. Here planar stratified minerogenic silty sand is interstratified with layers of dense mats of plant remains, up to 15 mm thick.

The organic remains were dominated by aquatic reed species, and in places macroscopic remains of *Salix herbacea* and *Betula nana*.

LF3b is an orange-brown crudely to well-stratified matrix-supported sand and gravel, interstratified with thin (~2 cm) facies of coarse, clast-supported gravel, coarse sand, and silt. Gravels are planar stratified, offlapping to the south-southeast at 6-37° and in places display a lensate, channel-like morphology (Figures 14 and 16). Interstratified silts often show distinct loading structures; convolution, flames, and pipes. Facies thickness varies, with areas of thin (~5 cm) silty sand facies interstratified with thick (>30 cm) facies of gravel. The matrix is dominated by coarse to medium sand (~700-900 µm in Tasiussaq and 400 µm in Arfertuarssuk). Pebble to cobble sized clasts are sub-angular to sub-rounded local basaltic lithologies, with C40 values of 36 - 64%, and RA values of 10 - 44 (Figures 10 and 11), suggestive of blocky, compact, sub-rounded clasts. Rare shell fragments were found throughout LF3b, but no whole shells were retrieved. In Log 10 (Ulissat), a 2.5 m section of matrix supported gravel contained large-scale cross-cutting lenticular geometry. In Log 8, LF3b displayed a distinct fining upwards sequence, with a marked reduction in clast size and density, accompanied by an increase in bedding dip.

LF3c is composed of well to very-well sorted interstratified clayey silts, fine to coarse sand, and fine sand and gravel. Units are horizontally planar stratified and up to 50 cm thick. Granule sized clasts are local basalt and appear sub-angular to sub-rounded. No clast form data was taken from this lithofacies. In Log 10 (Ulissat), a 2.5 m section of matrix supported gravel contained well-developed, large-scale cross-cutting lenticular geometry (Figure 14).

5.2.4. LFA4

LFA4 is a moderately to poorly stratified, medium to coarse, planar stratified sand and gravel. The bulk of LFA4 is matrix supported, although infrequent facies of clast supported gravels were logged. Facies from LFA4 dip variably throughout Svartenhuk Halvø: south-southeast at 20-38° in Arfertuarssuk, and west at 8-20° in Tasiussaq. Gravelly facies in Log 3 are interstratified with fine grained facies of beige sandy silt, and discontinuous lenses of brown silty clay. These contain angular basaltic granules up to 3 cm in diameter. Clasts are local basaltic lithologies, pebble to cobble sized, and angular to rounded. The clasts returned C40 values of 60 - 64% and RA values of 55 - 65 (Figures 10 and 11).

5.2.5. LFA5

LF5a is a grey to pink-grey, massive, matrix-supported diamicton. It is moderately to well consolidated, with a bimodal matrix distribution, with modes at 1000 µm (coarse sand) and 45 µm (coarse silt). The matrix is rich in marine shells, with common fragments and rare intact *in-situ* single valves. In places the shells are held in

distinct horizons. The contact between LFA5 and underlying lithofacies is very sharp with no evidence of sediment mixing. Clasts in LF5a are local basaltic lithologies, up to 20 cm in diameter and sub-angular to sub-rounded, 15% of which are striated. Clast fabrics are moderately to strongly clustered, displaying low isotropy (Figures 11). The macrofabric data return an S1 eigenvalue of 0.59, suggesting moderate to high a-axis clustering, and a girdle to moderate cluster clast form shape (Figure 10). Clast form analysis is clustered toward blocky and elongate, and data show C40 values of 38-48%, and a highly variable RA of 6-56 (Figures 10 and 11). As with LFA2, the lithofacies contained abundant marine shell fragments, with very rare paired valves. A paired valve was sampled from the sediment for radiocarbon dating, and returned a finite age of 44.8 cal. kyr BP (Table 4).

LF5b was recorded capping Logs 7 and 8 in Tasiussaq. This lithofacies is characterised by up to 1 m of yellow, clast supported sandy gravel, in places becoming open framework. The facies is generally structureless, with some very crude sub-horizontal stratification. In Log 7, the gravel is interstratified with occasional lenses (~3 cm thick) of well-consolidated pink diamicton, of identical colour, texture, and grain size to LF5a. Clasts are local basaltic lithologies, up to ~14 cm in diameter, and dominated sub-rounded and rounded clasts. Clast form data show C40 values of 26-32%, and RA values 14-20 (Figures 10 and 11), reflecting an active transport history, either through subglacial or englacial pathways (Benn and Evans, 2010).

5.3. Interpretation

5.3.1. LFA1

The brecciated bedrock of lithofacies association LFA1 is interpreted as heavily weathered, glacio-tectonised *in-situ* bedrock, and is indicative of overriding by grounded, warm-based glacier ice. Modification would have occurred during an extended period of periglacial, cold-climate conditions. Initial bedrock brecciation is likely to have been caused by ground ice development during prolonged periglacial conditions (Murton, 1996). However, the interfingering of zones of brecciated bedrock with bedrock-rich diamicton (Figures 12 and 15) suggests formation and bedrock disturbance through glaciotectonism under a warm-based ice mass (Harris, 1991; Phillips et al., 2013). The transition from undeformed bedrock (via heavily brecciated bedrock) to a clast- to matrix-supported diamict is a result of a change in process through time and has been reported elsewhere (Benn and Evans, 1996; Croot and Sims, 1996; Hiemstra et al., 2007). The diamictic lithofacies both above this bedrock (and in places interstratified with it) is produced by more intense glaciotectonic processes, including bedrock crushing and mixing with fine rock flour (Goldthwait and Matsch, 1989; Hiemstra et al., 2007). The lowermost bedrock which varies between intact and brecciated is the result of minor glaciotectonic activity. It is also possible that the overlying LFA2 is a glaciotectonite, forming the final facies within this transitional sequence from glaciotectonic action to subglacial erosion.

5.3.2. LFA2

LFA2 displays many sedimentological, structural and clast properties of a hybrid subglacial till, formed through deformation and lodgement (Evans et al., 2006). These include a poor to well-consolidated diamictic matrix, with sub-rounded, lodged, striated clasts. The thick nature of LFA2 (up to 5 m) may be due to lodgement and reworking of pre-existing sediment, including till (Dowdeswell and Sharp, 1986; Evans et al., 2006), or due to ice-marginal processes (folding, thrusting and stacking), which lead to till thickening (Evans and Hiemstra, 2005; Ó Cofaigh et al., 2011). It is possible that the massive, structureless nature of LFA2 is due to sediment homogenisation through high levels of strain and sediment mixing (Boulton and Jones, 1979; van der Wateren, 1995), or is partially inherited from pre-existing sediment. Clasts are all local basaltic lithologies, suggesting glacial erosion and incorporation of basaltic bedrock from the Svartenhuk Halvø interior into LFA2, prior to emplacement. The presence of abundant shell fragments throughout the facies suggests the glacier reworked local pre-existing marine sediment during till genesis. The rare interbedded stratified diamicton could relate to part of the continuum from a stratified to massive diamict, which would be indicative of progressive homogenisation through mixing (Evans et al., 2006; Ó Cofaigh et al., 2011). Clast fabric data support the interpretation of LFA2 as a subglacial till. The data show low isotropy and variable elongation, falling within known envelopes of upper till fabric, suggesting clast emplacement through lodgement and non-solid state deformation (Benn, 1994; Bennett et al., 1999). In places, clast fabric data are highly bimodal (see Log 2; Figure 12), with a secondary modal peak transverse to the direction of ice-flow reconstructed from bedrock striae evidence. This bimodality could be the result of a localised increase in lodgement, aligning clasts transverse to flow (Andrews and Shimizu, 1966; Lindsay, 1970), or could be the result of weakly constrained deformation (Hicock, 1992; Hicock and Fuller, 1995). Given the multimodal fabric from Log 1, the latter appears more likely. Directional clast fabric data suggest ice flow from the north-northwest, in agreement with striae data from bedrock within the fjord. The relatively weakly clustered clast fabrics suggest ductile deformation similar to the upper A horizons of tills in Iceland (Evans et al., 2006). In places clast fabrics show no preferential orientation. This is likely to be a result of a localised decrease in the strain experienced by the sediment (Benn, 1995), or a function of the thick deforming layer (Hart, 1994). Clast form covariance data reveal a relatively angular clast assemblage (Figures 10 and 11), suggesting a short clast transport distance.

5.3.3. LFA3

Based upon both their sedimentology (bottomsets, foresets, and topsets) and geomorphology (flat topped features with sloping front and rear faces) LFA3 is interpreted as Gilbert-type deltas (Bates, 1953; Benn and Evans, 2010; Gilbert, 1885). Gilbert-type deltas form in both glacier-fed and ice-contact settings (Benn and Evans, 2010), and often display very similar sedimentological properties (Lønne, 1993). The raised deltas from which Logs 4 (centre of the Arfertuarssuk Fjord) and 10 (Ulissat valley) were recorded are distinct features with steeply sloping upstream flanks, lower angle downstream slopes, and no upstream continuation. These

upstream slopes are interpreted as ice-contact slopes, providing evidence that the delta was ice-contact during its formation. In contrast, the delta from which Logs 1-3 were recorded, at the head of Arfertuarssuk Fjord, does not display a clear ice-contact slope, and is tentatively interpreted as glacier-fed. Similarly, the deltas from which Logs 6-9 were recorded do not display clear ice-contact slopes, and as a result can only be classified as Gilbert-type deltas, and not as glacier-fed or ice-contact.

The fine-grained planar stratified deposits of LF3a are interpreted as bottomsets of a delta, representing low-energy fluviodeltaic sedimentation (Gilbert, 1885; Lønne, 1995), deposited by suspended-load sediment settling in front of an advancing delta (Gilbert, 1885; Kenyon and Turcotte, 1985; Lønne, 1995). The ubiquitous macroscopic plant remains are likely to have been introduced from upstream regions, indicative of either a period of ice-free conditions sufficient to allow vegetation growth and inwash, or reworking of pre-existing vegetation during glacial advance. The coarsening upwards sequence noted within LF3a suggests a progressive increase in the proximity of the ice margin to the location of deposition.

LF3b is interpreted as a sequence of gravelly glaciogenic delta forests (Edwards, 1986; Gilbert, 1885; Nemec and Steel, 1984), deposited in a marine environment. The poor sorting and weak clast imbrication within foreset beds reflects deposition through avalanching, highly concentrated debris flows, and bedload deposition down the delta face (Kenyon and Turcotte, 1985; Postma and Roep, 1985). The upward fining sequence recorded in LF3b from Tasiussaq are common sedimentological characteristics of delta foresets (Clemmensen and Houmark-Nielsen, 1981), representing retreat of the ice margin. In contrast, the exposure of LF3b found at the head of Arfertuarssuk (Log 1 and 2) is characterised by a coarsening upwards sequence. It is possible that this is due to deposition proximal to a glacier meltwater efflux (Bannerjee and McDonald, 1975; Cheel and Rust, 1982), or glacier margin advance. The inferred direction of delta formation from foreset dip varies between valleys, with deposition from the north in Arfertuarssuk and Ulissat, and the east in Tasiussaq. Clast form data are variable throughout logged exposures of the lithofacies, but suggest active transport. C40 and RA values are higher than those reported from other deltaic deposits, suggesting a short transport history, and limited clast rounding (Benn and Evans, 1993).

LF3c is a massive to planar interstratified silt to gravel and is interpreted as low energy glaciolacustrine and glaciofluvial deposits, formed in the proglacial zone as delta topsets. Variations in grain size and sediment texture is a function of water depth (Fyfe, 1990) and glacier proximity. The low energy nature of the sediments suggest deposition occurred in an ice-distal setting. Although LFA3 is found extensively throughout Arfertuarssuk, Tasiussaq, exposure of LF3c is restricted, only found in Logs 6 and 10. The well-developed lenticular geometry of sediments in Log 10 records the development of palaeochannels, a common feature of

topset deposits (Fyfe, 1990; Lønne and Nemec, 2004), providing evidence for the development of well-defined, channelised flow across the delta surface.

5.3.4. LFA4

Based upon the dipping stratification, and frequent sharp switches between matrix and clast supported facies, LFA4 is interpreted as a stratified slope deposit (DeWolf, 1988; Francou, 1990). These deposits are likely to have formed through gravitationally driven slope wash, debris flow, and solifluction (Bertran et al., 1997), sourced from steep terrain backing a number of delta sites. Stratification and a clear sorted structure are indicative of an overland flow component (Bertran and Texier, 1999). The repeatable pattern of switches between matrix-rich gravel and layers of coarser clast-rich gravel is characteristic of stratified slope deposits, formed through multiple stacked grain flows (Van Steijn et al., 2002). Clast form data support this interpretation, with the highest C40 and RA values reported from this study. The C40 – RA plot places the LFA4 samples in a similar region to previously reported scree and supraglacial material (Benn and Ballantyne, 1994) (Figure 11). Such high angularity is characteristic of slope deposits, with a relatively short, passive transport pathway (Ballantyne, 1982; van Steijn, 1996; Van Steijn et al., 2002). These data suggest a preference to slabby, elongate forms, also indicative of unmodified, frost-weathered clast (Ballantyne, 1982). The presence of interstratified fines throughout LFA4 suggests some input through slope wash.

5.3.5. LFA5

Based upon its diamictic nature, moderate to strong clustering of clast fabric coincident with independent indicators of ice flow direction, and the presence of striated clasts, LF5a is interpreted as a moderately to well-consolidated subglacial till. The presence of local basaltic clasts and shell fragments throughout LF5a suggests both erosion of the underlying basaltic bedrock and cannibalisation of pre-existing localised marine sediments. Clast form data display a higher C40 value than previously reported subglacial tills (Benn and Ballantyne, 1994), although the low RA values are similar. The high angularity of clasts in comparison to other studies could be due to short transport distance, as in LFA2. Clast fabric data support the interpretation of LF5a as a subglacial till, showing low isotropy and moderate to high elongation; falling within known envelopes of till fabric (Benn, 1994; Bennett et al., 1999). The strength and direction of preferential clast orientation varies between logged facies, but orientation is in agreement with independent ice flow indicators, inferring north-northwest to south east ice flow in Arfertuarssuk, and northeast to southwest ice flow in Tasiussaq. When LF5a is found in association with LFA2, clast macrofabrics from both lithofacies are in agreement, suggesting multiple overriding ice advances from similar directions. Fabric from the lower portion of LF5a in Log 7 is multimodal, possibly relating to a localised decrease in the strain experienced by the sediment (Benn, 1995), or a function of a thick deforming bed allowing free rotation of clasts (Evans et al., 2006; Hart, 1994; Hicock, 1992). The absence of any

bedding or deformation structures could suggest sediment homogenisation through mixing (van der Wateren, 1995), or alternatively could simply be a primary sedimentary characteristic of a partially reworked deposit.

Exposures of LF5b are only found in locations where eskers were found on the land surface (see Section 4.1.2.). As a result, the LF5b sand and gravel is interpreted as esker fill gravel (Benn and Evans, 2010; Warren and Ashley, 1994).

6. Discussion

6.1. Geomorphological and sedimentological evidence for glaciation of southern Svartenhuk Halvø

Within the interior of Svartenhuk Halvø only discrete, small-scale evidence of ice activity was found, including small, subdued lateral moraines, fragmentary eskers, and occasional edge-rounded erractic boulders perched upon the landsurface, and overspill channels, the latter formed through drainage of glacier dammed lakes. Evidence for glacial alteration of high-level land surfaces to the east of Arfertuarssuk and north and southeast of Tasiussaq is present but minor, with erratics and rare striated surfaces above 300 m a.s.l. Heavily weathered, high-altitude surfaces display evidence of a long-term surface exposure history, suggesting the area has been covered by thin, protective, cold-based ice (Rea and Evans, 2003) sourced from high-level plateaux. This protective ice cover is likely to have developed during both the LGM and previous glacial periods, although at present there is no chronological control on the exposure history of the surface.

Glacially striated bedrock at present sea level, lateral moraines, and eskers provide convincing geomorphological evidence for the expansion of locally sourced valley glaciers to the present coastline in Arfertuarssuk and Tasiussaq. Terminal positions of these glaciers are unknown, although geomorphological evidence constrains them to a position at least offshore of the present coastline. Alongside this, glaciogenic deltas (both ice-contact and glacier-fed) and areas of kettled outwash record the deglaciation of valley glaciers from the coastline. The presence of glaciogenic deltas is suggestive of a retreating glacier front, punctuated episodically by stillstands. The geomorphology of kettled outwash and its stratigraphic position above the glaciogenic deltas in Arfertuarssuk and Tasiussaq suggests that these surfaces represent the final stages of the deglaciation from southern Svartenhuk Halvø, likely to have been formed by valley glaciers with debris charged snouts, causing ice burial and stagnation during withdrawal (Benn and Evans, 2010).

Deposits interpreted as subglacial till (LFA2 and LF5a) are found extensively throughout Arfertuarssuk (Logs 1 and 2) and Tasiussaq (Logs 5, 6, and 9), providing direct evidence for grounded, warm-based ice. Further evidence for local glaciation is provided by bedrock and sediments displaying evidence of glaciotectonic deformation (LFA1 – Log 5). Clast fabric data from subglacial tills are in agreement with bedrock striae, moraine and delta orientation, suggesting that flow was topographically confined by valley morphology, with ice sourced

from the high-altitude centre of the Svartenhuk Halvø, with no input from the GrIS. In Arfertuarssuk, the exposure of LFA2 and LF5a within a single section provides evidence for two distinct ice advances in Arfertuarssuk. In contrast, although both LFA2 and LF5a are present in Tasiussaq, they were not found in a single stratigraphic section. The presence of whole and fragmented marine shells in LFA2 and LF5a suggests that the sediments were either originally deposited during a higher than present sea-level, or consist of reworked marine sediments. Due to the absence of sedimentary criteria diagnostic of glaciomarine deposition (see Hart and Roberts, 1994), the reworking of pre-existing marine sediment is deemed most likely. Proglacial sediments are found between the subglacial tills, recording a period of proglacial delta formation. These provide evidence for periods of ice retreat in Arfertuarssuk, Tasiussaq, and Ulissat, during which delta development occurred. The presence of whole and fragmentary marine shells throughout LFA3 and the *in situ* nature of the sediments suggests deposition and delta formation occurred under marine conditions. This is supported by delta and alluvial fan geomorphology from the Svartenhuk Halvø coast, which is graded to a series of heights above sea-level (12 – 75 m a.s.l.), inferring formation during a higher than present relative sea-level.

6.2. Chronology of southern Svartenhuk Halvø deposits

The existing chronology constraining the deposits analysed in this study is based upon a number of infinite (>40 kyr) radiocarbon ages from sites close to Logs 1, 3, and 5/6 (Table 1), amino acid racemisation determinations, and U-series ages (>89 and 115 kyr BP (no errors quoted) - Funder et al., 1994 as from Kelly, 1986), suggesting pre-LGM sediment deposition. Despite the stark disagreement in the sedimentological interpretations presented by this study and the studies from which the dates originate, the chronological control remains valid. This study has provided an additional two dates from Arfertuarssuk (Log 1 - Table 4), both of which returned ages of 47.7 cal. kyr BP and 44.8 cal. kyr BP. It should be noted that it is possible that these ages are, however, non-finite. As outlined in detail by Mangerud et al. (2008), samples this old are sensitive to contamination by younger ^{14}C, and found that high D/L values indicated that some ages in the rage 48-43 cal. kyr BP could instead be considered as non-finite. At present, the small number of new ages and infinite values of older ages makes a robust validation of the Svartenhuk chronology impossible. However, a number of observations can be drawn from the data. Unless these dates represent large underestimates of shell age, or are actually non-finite, they are in disagreement with the current proposed age of deposition for the sediments (MIS 5 - Bennike et al., 1994; Funder et al., 1991; Kelly, 1986). The majority of published radiocarbon ages which have been used to constrain the age of deposits produced non-finite ages of >30.4 to >40 cal. kyr BP (Table 2), in which the shell signal was not discernible from background. However, recent progress in the precision of measurements and the use of AMS makes it possible that rerunning of these samples would now return a finite measurement. The new shell ages, taken from a subglacial till of a possibly reworked assemblage therefore provide a *maximum* age for the emplacement of the subglacial till, and consequently the glacier advance. The highly crushed nature of the shell assemblage within LFA2 and LF5a provides some evidence of post-depositional sediment reworking during

subsequent glacial activity. This makes it possible that the shells dated from Svartenhuk Halvø, although dating shell formation, are not dating sediment deposition.

The sparse chronology across southern Svartenhuk Halvø makes correlation between sites, and indeed individual valley systems difficult. As no new dates were produced for Tasiussaq or Ulissat, they remain undated. Further chronological control from all three valleys would assist in correlation, however the similar geomorphology, sedimentology, stratigraphy, and hypothesised source region (the high-altitude Svartenhuk Halvø interior) suggests that lithofacies found at multiple sites *were* deposited during the same phase of glacial activity (i.e. the LGM). The present chronology also makes understanding the presence of multiple subglacial tills difficult. Where found, they are consistently separated by LFA3, suggesting a distinct period of ice retreat before the second phase of overrunning and deposition of LF5a. Further constraint upon age of deposition could be provided by the relative height of deposits throughout southern Svartenhuk Halvø. The deposits are graded to a number of distinct levels above present sea-level, and the presence of marine fauna within the deposits indicates their deposition in a marine setting at a time with a higher than present sea-level, or the reworking of previously deposited marine sediment by subsequent glacial advance. The *in situ* LFA3 is thought to have been deposited during a period of ice retreat, into a higher than present relative sea-level.

No local relative sea-level curve exists for the Svartenhuk Halvø or Uummannaq region, but the local marine limit from this study (75 m a.s.l.) appears in good agreement with both isolation basin studies from Arveprinsen Ejland in Disko Bugt (Long et al., 1999) and modelling results from the Uummannaq region (Lecavalier et al., 2014). At present no Holocene raised marine deposits have been dated on Svartenhuk Halvø, despite their prevalence in Disko Bugt. This is likely due to a difference in glacial histories of the regions, as Svartenhuk Halvø is thought to have been covered by extensive local glaciers during the LGM, not the GrIS.

6.3. Implications for regional ice sheet history

Through remote mapping and extensive ground-truthing, both geomorphological and sedimentological data demonstrate glaciation of the peninsula to the present coastline. This is in clear contrast to previous studies which have only reported evidence for restricted valley glaciation, leaving little-to-no imprint on the landscape. The findings provide compelling evidence for glacier expansion to the present coastline, and its subsequent retreat to the Svartenhuk Halvø interior. Based upon ice flow indicators and clast lithological composition, these glaciers are thought to have been sourced from high altitude plateaux in central Svartenhuk Halvø. Glaciation of the peninsula is characterised by large valley glaciers which are likely to have been sourced from high-level ice fields. The geomorphological signal of glaciation is patchy and subtle, and is likely to be a product of both ice cap and valley glacier build up over the high and low elevation areas respectively. Both forms of ice build-up leave a variety of geomorphological imprints upon the landscape, dependent on their thermal regime, extent,

628 and timing. More detailed study of the entire peninsula is required in order to fully characterise the precise
629 mode of locally sourced glaciation this region experienced.
630
631 Very little evidence exists for the presence of any widespread ice sheet or ice stream activity within any of the
632 valleys studied. This suggests that the large UIS did not move on-shore in southern Svartenhuk Halvø either
633 during or following the deposition of the sediments throughout southern Svartenhuk Halvø. This absence of
634 ice stream impact upon a very low-lying coastal area, in close proximity is due to a number of reasons. Firstly,
635 given the westerly position of the Svartenhuk Halvø (50.00°W to 55.00°W), land is likely to have been fed by
636 moisture-rich air from Baffin Bay. During glacial periods this would have encouraged rapid, widespread ice
637 development on the high elevation areas of Svartenhuk Halvø. This rapid ice build-up during the onset of full
638 glacial conditions would have protected the region from the GrIS as the UIS developed. In conjunction with the
639 shallow bathymetry to the north of Ubekendt Ejland, protective local ice prevented any areal scour of the
640 Svartenhuk Halvø region by the GrIS, and would have helped to encourage the development of the UIS, by
641 forcing northern outlet glaciers southwards into the Uummannaq trough. Thus, the tentative correlation of
642 deposits to the last glacial cycle is supported by the hypothesised configuration of the UIS during the LGM (Ó
643 Cofaigh et al., 2013b; Roberts et al., 2013) as it is unlikely that pre-LGM sediments would have survived through
644 the LGM within large, low elevation valleys. Although a systematic analysis of the entire peninsula was not
645 undertaken, glacial activity across Svartenhuk Halvø is likely to have been characterised by a patchwork of
646 mountain valley glaciers and protective cold-based plateaux. The presence of this large system of ice caps and
647 mountain valley systems is not uncommon throughout Greenland, many of which can be seen today. However,
648 their expansion to the present coastline at a time thought to represent full-glacial conditions is unusual in West
649 Greenland, and appears to be a unique result of the topographic configuration of the Uummannaq region.
650
651 Geomorphological and sedimentological evidence from southern Svartenhuk Halvø also provide plentiful
652 evidence for higher than present relative sea-levels, from 12 to 75 m a.s.l. This was recognised by previous
653 studies and used to infer the deposition of sediments during previous periods of interglacial conditions (Funder
654 et al., 1994). Though previous interglacials would have been periods of high relative sea-level, post-LGM sea-
655 level in this region is thought to have reached sufficient heights to produce the features found in this study.
656
657 Results from this study have implications for the SME, originally interpreted from these sediments and dated to
658 MIS 5 (Bennike et al., 1994; Kelly, 1986). This event is thought to be associated with warm temperatures and an
659 elevated relative sea-level during the last interglacial. Based on the geomorphological, sedimentological, and
660 chronological evidence, and the resulting glacial history presented in this study, this event is untenable. These
661 results present a different interpretation of the sediments found throughout the Svartenhuk Halvø coast. As
662 argued above, a number of the deposits are clearly glacial in origin, in disagreement with previous studies

(Bennike et al., 1994; Kelly, 1986). Though previous workers have identified some sedimentological evidence for glacial activity (Funder et al., 1994), this study has reported it far more widely. In addition, evidence for glaciation was found *both* below and above the sediments formerly ascribed to the SME. Given that radiocarbon shell ages of similar age 44.8 – 47.7 cal. ka BP were obtained from reworked shells in both LFA2 and LF5a, it makes the assertion that the intermediate sediments (LFA3 and LFA4) are from MIS5 highly unlikely. It is possible that the SME does exist, however the deposits analysed in this study provide no evidence to support this. The alternative interpretation presented here also helps to explain the micro- and macro-faunal assemblages (Bennike et al., 1994).

Though this work has provided a solid sedimentological and geomorphological context for the sediments, further chronological control upon the deposits is needed in order to fully understand the depositional history of the coastline, and to robustly correlate between the three valleys studied.

7. Conclusions

Morphosedimentary investigation of deposits from three valleys in southern Svartenhuk Halvø has produced compelling evidence for the expansion of warm-based glaciers to the present coastline in the past. These findings are in direct disagreement with sedimentological results from previous research in the Svartenhuk Halvø region. These studies investigated some of the same sediments to this study, and interpreted them as pre-LGM, littoral marine sediments, with little/no evidence of glacial activity. As a result the SME was proposed (Bennike et al., 1994; Funder et al., 1991; Kelly, 1986). Although evidence was found for marine depositional environments, sedimentological results provide evidence for deposition within fluvial, glaciofluvial, and subglacial environments, close to present sea-level. These deposits have formed a series of ice-contact and glacier-fed deltas, alluvial fans, and kettled outwash surfaces which, in places, appear to have been graded to a high relative sea-level.

The chronological control from Arfertuarssuk Fjord is also contrary to previous work, which constrained the deposition of the SME to MIS 5. Two new shell dates from the lower and upper subglacial tills in Arfertuarssuk returned ages which provide a maximum age of 49.8 cal. kyr BP for till emplacement, and therefore glacial advance. This places maximum age of the most recent glaciation of Arfertuarssuk, and potentially the entire southern Svartenhuk Halvø coast, within MIS 3. It is possible that the marine fauna within the subglacial tills could represent a heavily reworked assemblage, and therefore the dates presented here represent an age over-estimation. As a result, the glaciation of Arfertuarssuk is tentatively correlated to the last glacial cycle, although it may represent an advance prior to the LGM in Greenland. No new chronological control could be provided for Tasiussaq or Ulissat, and as a result they remain undated within this framework. However, further radiocarbon and surface exposure (^{36}Cl) are forthcoming. These will provide a more rigorous age control upon

the glaciation of the southern Svartenhuk Halvø coast. Deposits and landforms record widespread glacier retreat and a series of marginal oscillations during deglaciation. This area is therefore unique in West Greenland, where due to ice sheet cover; few areas contain evidence for independent valley glaciation. Further detailed investigation of other valleys and areas across Svartenhuk Halvø could provide important information about the way in which glaciers not coupled with the main ice sheet responded to changes in climate, ocean temperature, and neighbouring ice sheet and ice stream extent.

Acknowledgments

This work was supported by the Department of Geography (Durham University), the Department of Geography and the Environment (University of Aberdeen), the RGS-IBG, and a NERC Radiocarbon Facility Grant. Thanks to Arne Neumann, Birte Ørum, and Barbara Stroem-Baris for logistical support, and to NERC Radiocarbon Facility staff for the preparation of radiocarbon samples.

713 Andrews, J.T., Shimizu, K., 1966. Threedimensional vector technique for analyzing till fabrics:
714 Discussion and FORTRAN program. Geological Bulletin 8, 151-165.
715 Ballantyne, C.K., 1982. Aggregate clast form characteristics of deposits near the margins of four
716 glaciers in the Jotunheimen Massif, Norway. 103-113.
717 Bannerjee, I., McDonald, B.C., 1975. Nature of esker sedimentation, in: Jopling, A.V., McDonald,
718 B.C. (Eds.), Glaciofluvial and Glaciolacustrine Sedimentation. . SEPM Special Publications 23, pp.
719 132-154.
720 Bates, C.C., 1953. Rational theory of delta formation. American Association of Petroleum Geologists
721 Bulletin 37, 2119-2161.
722 Benn, D., Evans, D.J.A., 2010. Glaciers and Glaciation., 2 ed. Hodder Education, London.
723 Benn, D.I., 1994. Fabric Shape and the Interpretation of Sedimentary Fabric Data Journal of
724 Sedimentary Research, Section A: Sedimentary Petrology and Processes 64A, 910-915.
725 Benn, D.I., 1995. Fabric signature of till deformation, Breiðamerkurjökull, Iceland. Sedimentology
726 42, 735-747.
727 Benn, D.I., Ballantyne, C.K., 1994. Reconstructing the transport history of glacigenic sediments: a
728 new approach based on the co-variance of clast form indices. Sedimentary Geology 91, 215-227.
729 Benn, D.I., Evans, D.J.A., 1993. Glaciomarine deltaic deposition and ice-marginal tectonics: The
730 'Loch Don Sand Moraine', Isle of Mull, Scotland. Journal of Quaternary Science 8, 279-291.
731 Benn, D.I., Evans, D.J.A., 1996. The interpretation and classification of subglacially-deformed
732 materials. Quaternary Science Reviews 15, 23-52.
733 Bennett, M.R., Waller, R.I., Glasser, N.F., Hambrey, M.J., Huddart, D., 1999. Glacigenic clast fabric:
734 genetic fingerprint or wishful thinking? Journal of Quaternary Science 14, 11.
735 Bennike, O., Hansen, K.B., Knudsen, K.L., Penney, D.N., Rasmussen, K.L., 1994. Quaternary Marine
736 Stratigraphy and Geochronology in Central West Greenland. Boreas 23, 194-215.
737 Bertran, P., HÉTu, B., Texier, J.-P., Van Steijn, H., 1997. Fabric characteristics of subaerial slope
738 deposits. Sedimentology 44, 1-16.
739 Bertran, P., Texier, J.-P., 1999. Facies and microfacies of slope deposits. CATENA 35, 99-121.
740 Boulton, G., Eyles, N., 1979. Sedimentation by valley glaciers: a model and genetic classification.
741 Moraines and varves 33, 11-23.
742 Boulton, G.S., Jones, A.S., 1979. Stability of temperate ice caps and ice sheets resting on beds of
743 deformable sediment. Journal of Glaciology 24, 29-43.
744 Briner, J.P., Kaufman, D.S., Bennike, O., Kosnik, M.A., 2014. Amino acid ratios in reworked marine
745 bivalve shells constrain Greenland Ice Sheet history during the Holocene. Geology 42, 75-78.
746 Bull, W., 1977. The alluvial fan environment. Progress in Physical Geography 1, 49.
747 Cheel, R.J., Rust, B.R., 1982. Coarse grained facies of glaciomarine depositis near Ottawa, Canada,
748 in: Davidson-Arnott, R., W., N., Fahey, B.D. (Eds.), Research in Glaciofluvial and Glaciolacustrine
749 Systems. Geobooks, Norwich.
750 Clemmensen, L.B., Houmark-Nielsen, M., 1981. Sedimentary features of a Weichselian
751 glaciolacustrine delta. Boreas 10, 229-245.
752 Croot, D.G., Sims, P.C., 1996. Early stages of till genesis: an example from Fanore, County Clare,
753 Ireland. Boreas 25, 37-46.
754 Dahl-Jensen, D., Albert, M., Aldahan, A., Azuma, N., Balslev-Clausen, D., Baumgartner, M., Berggren,
755 A.-M., Bigler, M., Binder, T., Blunier, T., 2013. Eemian interglacial reconstructed from a Greenland
756 folded ice core. Nature 493, 489-494.
757 DeWolf, Y., 1988. Stratified slope deposits, in: Clark, M.J. (Ed.), Advances in Periglacial
758 Geomorphology. Wiley, Chichester, pp. 91-110.

759 Dowdeswell, J., Hogan, K., Ó Cofaigh, C., Fugelli, E., Evans, J., Noormets, R., 2014. Late Quaternary
760 ice flow in a West Greenland fjord and cross-shelf trough system: submarine landforms from Rink
761 Isbrae to Uummannaq shelf and slope. Quaternary Science Reviews 92, 292-309.
762 Dowdeswell, J.A., Sharp, M.J., 1986. Characterization of pebble fabrics in modern terrestrial
763 glacigenic sediments. Sedimentology 33, 699-710.
764 Edwards, M.B., 1986. Glacial Environments, in: H.G., R. (Ed.), Sedimentary Environments and Facies.
765 Blackwell, Oxford, pp. 416-438.
766 Evans, D.J.A., Benn, D.I., 2004. A practical guide to the study of glacial sediments. Arnold, London.
767 Evans, D.J.A., Hiemstra, J.F., 2005. Till deposition by glacier submarginal, incremental thickening.
768 Earth Surface Processes and Landforms 30, 1633-1662.
769 Evans, D.J.A., Phillips, E.R., Hiemstra, J.F., Auton, C.A., 2006. Subglacial till: Formation, sedimentary
770 characteristics and classification. Earth-Science Reviews 78, 115-176.
771 Francou, B., 1990. Stratification mechanisms in slope deposits in high subequatorial mountains.
772 Permafrost and Periglacial Processes 1, 249-263.
773 Funder, S., 1989. The Baffin-Bay Region during the Last Interglaciation - Evidence from Northwest
774 Greenland. Geographie Physique Et Quaternaire, Vol 43, No 3, 255-262.
775 Funder, S., Hjort, C., Kelly, M., 1991. Isotope stage 5 (130-74 ka) in Greenland, a review. Quaternary
776 International 10–12, 107-122.
777 Funder, S., Hjort, C., Landvik, J.Y., 1994. The Last Glacial Cycles in East Greenland, an Overview.
778 Boreas 23, 283-293.
779 Funder, S., Kjeldsen, K.K., Kjær, K.H., Ó Cofaigh, C., 2011. The Greenland Ice Sheet During the Past
780 300,000 Years: A Review, in: Ehlers, J., Gibbard, P.L., Hughes, P.D. (Eds.), Quaternary Glaciations -
781 Extent and Chronology: A Closer Look. Elsevier, Oxford, pp. 699-713.
782 Fyfe, G.F., 1990. The effect of water depth on ice-proximal glaciolacustrine sedimentation:
783 Salpausselka I, southern Finland. Boreas 19, 18.
784 Gelting, P., 1934. Studies on the vascular plants of East Greenland between Franz Joseph Fjord and
785 Dove Bay. Meddelelser om Gronland 101.
786 Gilbert, G.K., 1885. The topographic features of lake shores. U.S. Geological Survey Annual
787 Report 5, 49.
788 Goldthwait, R.P., Matsch, C.L., 1989. Genetic classification of glacigenic deposits.
789 Goossens, D., 2008. Techniques to measure grain‐size distributions of loamy sediments: a
790 comparative study of ten instruments for wet analysis. Sedimentology 55, 65-96.
791 Gustavson, T.C., Boothroyd, J.C., 1987. A depositional model for outwash, sediment sources, and
792 hydrologic characteristics, Malaspina Glacier, Alaska: A modern analog of the southeastern margin
793 of the Laurentide ice sheet. Geological Society of America Bulletin 99, 187-200.
794 Håkansson, L., Alexanderson, H., Hjort, C., Moller, P., Briner, J.P., Aldahan, A., Possnert, G., 2009.
795 Late Pleistocene glacial history of Jameson Land, central East Greenland, derived from cosmogenic
796 Be-10 and Al-26 exposure dating. Boreas 38, 244-260.
797 Harris, C., 1991. Glacial deposits at Wylfa Head, Anglesey, North Wales: Evidence for Late
798 Devensian deposition in a non-marine environment. Journal of Quaternary Science 6, 67-77.
799 Hart, J.K., 1994. Till fabric associated with deformable beds. Earth Surface Processes and Landforms
800 19, 18.
801 Henderson, G., Pulvertaft, T.C.R., 1987a. Descriptive text to geological map of Greenland 1:100 000,
802 Marmorilik 71 V.2 Agnete Syd, Nugatsiaq 71 V.2 Nord and Pangnertoˆq 72 V.2 Syd. Geol. Survey
803 Greenland, Copenhagen,.
804 Henderson, G., Pulvertaft, T.C.R., 1987b. Geological map of Greenland, 1:100 000, Mârmorilik 71
805 V.2 Syd, Nûgâtsiaq 71 V.2 Nord, Pangnertôq 72 V.2 Syd., in: Greenland, G.S.o. (Ed.), Copenhagen.

Henderson, G., Pulvertaft, T.C.R., 1987c. Geological map of Greenland, 1:100 000, Mârmorilik 71 V.2 Syd, Nûgâtsiaq 71 V.2 Nord, Pangnertôq 72 V.2 Syd. Descriptive text. Geological Survey of Greenland., Copenhagen.
Hicock, S.R., 1992. Lobal interactions and rheologic superposition in subglacial till near Bradtville, Ontario, Canada. Boreas 21, 73-88.
Hicock, S.R., Fuller, E.A., 1995. Lobal interactions, rheologic superposition, and implications for a Pleistocene ice stream on the continental shelf of British Columbia. Geomorphology 167-184.
Hiemstra, J.F., Evans, D.J.A., Cofaigh, C.O., 2007. The role of glacitectonic rafting and comminution in the production of subglacial tills: examples from southwest Ireland and Antarctica. Boreas 36, 386-399.
Kelly, M., 1986. Quaternary, pre-Holocene, marine events of western Greenland. Grønlands geologiske Undersøgelse 131, 23.
Kenyon, P.M., Turcotte, D.L., 1985. Morphology of a delta prograding by bulk sediment transport. Geological Society of America Bulletin 96, 1457-1465.
Kleman, J., Glasser, N.F., 2007. The subglacial thermal organisation (STO) of ice sheets. Quaternary Science Reviews 26, 585-597.
Lane, T.P., Roberts, D.H., Ó Cofaigh, C., Vieli, A., Rea, B., 2015. Glacial landscape evolution in the Uummannaq region, West Greenland. Boreas.
Lane, T.P., Roberts, D.H., Rea, B.R., Ó Cofaigh, C., Vieli, A., Rodés, A., 2014. Controls upon the Last Glacial Maximum deglaciation of the northern Uummannaq Ice Stream System, West Greenland. Quaternary Science Reviews 92, 324 - 344.
Laursen, D., 1944. Contributions to the Quaternary geology of northern West Greenland especially the raised marine deposits. Meddelelser om Gronland 135, 125.
Lecavalier, B.S., Milne, G.A., Simpson, M.J., Wake, L., Huybrechts, P., Tarasov, L., Kjeldsen, K.K., Funder, S., Long, A.J., Woodroffe, S., 2014. A model of Greenland ice sheet deglaciation constrained by observations of relative sea level and ice extent. Quaternary science reviews 102, 54-84.
Lindsay, J.F., 1970. Clast Fabric of Till and its Development. Journal of Sedimentary Research (SEPM) 40, 629-641.
Long, A.J., Roberts, D.H., Wright, M.R., 1999. Isolation basin stratigraphy and Holocene relative sea-level change on Arveprinsen Ejland, Disko Bugt, West Greenland. Journal of Quaternary Science 14, 323-345.
Lønne, I., 1993. Physical signatures of ice advance in a Younger Dryas ice-contact delta, Tromso, northern Norway: implications for glacier-terminus history. . Boreas 22, 12.
Lønne, I., 1995. Sedimentary facies and depositional architecture of ice-contact glaciomarine systems. Sedimentary Geology 98, 13-43.
Lønne, I., Nemec, W., 2004. High-arctic fan delta recording deglaciation and environment disequilibrium. Sedimentology 51, 553-589.
Lukas, S., Benn, D.I., Boston, C.M., Brook, M., Coray, S., Evans, D.J., Graf, A., Kellerer-Pirklbauer, A., Kirkbride, M.P., Krabbendam, M., 2013. Clast shape analysis and clast transport paths in glacial environments: A critical review of methods and the role of lithology. Earth-Science Reviews.
Maizels, J., 1992. Boulder Ring Structures Produced during Jökulhlaup Flows. Origin and Hydraulic Significance. Geografiska Annaler. Series A. Physical Geography, 21-33.
Maizels, J.K., 1977. Experiments on the origin of kettle-holes. Journal of Glaciology 18, 291-303.
Mangerud, J., Kaufman, D., Hansen, J., Svendsen, J.I., 2008. Ice‐free conditions in Novaya Zemlya 35 000–30 000 cal years BP, as indicated by radiocarbon ages and amino acid racemization evidence from marine molluscs. Polar Research 27, 187-208.

Murton, J.B., 1996. Near-surface brecciation of chalk, isle of thanet, south-east England: a comparison with ice-rich brecciated bedrocks in Canada and Spitsbergen. Permafrost and Periglacial Processes 7, 153-164.
Nemec, W., Steel, R.J., 1984. Alluvial and coastal conglomerates : Their significant features and some comments on gravelly mass-flow deposits., in: Koster, E.H., Steel, R.J. (Eds.), Sedimentology of Gravels and Conglomerates: Canadian Society of Petroleum Geologists, pp. 1-31.
Ó Cofaigh, C., Andrews, J.T., Jennings, A.E., Dowdeswell, J.A., Hogan, K.A., Kilfeather, A.A., Sheldon, C., 2013a. Glacimarine lithofacies, provenance, and depositional processes on a West Greenland trough-mouth fan. Journal of Quaternary Science 28, 13-26.
Ó Cofaigh, C., Dowdeswell, J.A., Jennings, A.E., Hogan, K.A., Kilfeather, A., Hiemstra, J.F., Noormets, R., Evans, J., McCarthy, D.J., Andrews, J.T., Lloyd, J.M., Moros, M., 2013b. An extensive and dynamic ice sheet on the West Greenland shelf during the last glacial cycle. Geology 41, 219-222.
Ó Cofaigh, C., Evans, D.J.A., Hiemstra, J.F., 2011. Formation of a stratified subglacial 'till' assemblage by ice-marginal thrusting and glacier overriding. Boreas 40, 1-14.
Phillips, E., Lee, J.R., Riding, J.B., Kendall, R., Hughes, L., 2013. Periglacial disruption and subsequent glacitectonic deformation of bedrock: an example from Anglesey, North Wales, UK. Proceedings of the Geologists' Association 124, 802-817.
Postma, G., Roep, T.B., 1985. Resedimented Conglomerates in the Bottomsets of Gilbert-type Gravel Deltas. Journal of Sedimentary Research (SEPM) 55, 12.
Price, R., 1970. Moraines at fjallsjökull, Iceland. Arctic and Alpine Research, 27-42.
Rea, B., Evans, D.J.A., 2003. Plateau Icefield Landsystem, in: Evans, D.J.A. (Ed.), Glacial Landsystems. Arnold, London.
Rich, J.L., 1943. Buried stagnant ice as a normal product of a progressively retreating glacier in a hilly region. American Journal of Science 241, 95-100.
Rink, H., 1853. Udsigt over Nordgronlands Geognosie. Kongelige danske Videnskabernes Selskabs Skrifter 5, 23.
Roberts, D.H., Long, A.J., Davies, B.J., Simpson, M.J.R., Schnabel, C., 2010. Ice stream influence on West Greenland Ice Sheet dynamics during the Last Glacial Maximum. Journal of Quaternary Science 25, 850-864.
Roberts, D.H., Long, A.J., Schnabel, C., Davies, B.J., Xu, S., Simpson, M.J.R., Huybrechts, P., 2009. Ice sheet extent and early deglacial history of the southwestern sector of the Greenland Ice Sheet. Quaternary Science Reviews 28, 2760-2773.
Roberts, D.H., Rea, B.R., Lane, T.P., Schnabel, C., Rodes, A., 2013. New constraints on Greenland ice sheet dynamics during the last glacial cycle: evidence from the Uummannaq ice stream system. Journal of Geophysical Research: Earth Surface 118, 23.
Sneed, E.D., Folk, R.L., 1958. Pebbles in the lower Colorado River, Texas a study in particle morphogenesis. The Journal of Geology, 114-150.
Sperazza, M., Moore, J.N., Hendrix, M.S., 2004. High-resolution particle size analysis of naturally occurring very fine-grained sediment through laser diffractometry. Journal of Sedimentary Research 74, 736-743.
Steenstrup, K.V.J., 1883. Om Forekomsten af Forsteninger i de kulførende Dannelser i Nord-Grønland. Meddelelser om Grønland 5, 43-67.
Sugden, D.E., 1974. Landscapes of glacial erosion in Greenland and their relationship to ice, topographic and bedrock conditions, in: Brown, E.H., Waters, R.S. (Eds.), Progress in Geomorphology: Papers in honour of David L. Linton. Institute of British Geographers Special Publication. No. 7. Institute of British Geographers, London, pp. 177-195.

Swift, D.A., Persano, C., Stuart, F.M., Gallagher, K., Whitham, A., 2008. A reassessment of the role of ice sheet glaciation in the long-term evolution of the East Greenland fjord region. Geomorphology 97, 109-125.
van der Wateren, F.M., 1995. Processes of glaciotectonism, in: Menzies, J. (Ed.), Modern Glacial Environments: Processes, Dynamics and Sediments. Butterworth-Heinemann, Oxford, pp. 309-335.
van Steijn, H., 1996. Debris-flow magnitude—frequency relationships for mountainous regions of Central and Northwest Europe. Geomorphology 15, 259-273.
Van Steijn, H., Boelhouwers, J., Harris, S., Hétu, B., 2002. Recent research on the nature, origin and climatic relations of blocky and stratified slope deposits. Progress in physical geography 26, 551-575.
Warren, W.P., Ashley, G.M., 1994. Origins of the ice-contact stratified ridges (eskers) of Ireland. Journal of Sedimentary Research 64, 433-449.
Whillans, I.M., 1978. Erosion by Continental Ice Sheets. The Journal of Geology 86, 9.

Table 1. List of locations logged in this study, their log number, and a reference if they have been studied by previous authors.

Log #	Site Name	Lat. (°N)	Long. (°W)	References (Site # in their text)
1	Arfertuarssuk fjord head 1	71.495	55.256	Bennike *et al*., 1994 (6); Kelly, 1986 (15)
2	Arfertuarssuk fjord head 1	71.495	55.256	Bennike *et al*., 1994 (6); Kelly, 1986 (15)
3	Arfertuarssuk fjord head 2	71.500	55.217	Bennike *et al*., 1994 (8)
4	Arfertuarssuk fjord side 1	71.468	55.168	Bennike *et al*., 1994 (9)
5	Kugssineq Coast	71.450	55.001	Bennike *et al*., 1994 (10); Kelly, 1986 (16); Laursen, 1944
6	Kugssineq Coast	71.450	55.001	Bennike *et al*., 1994 (10); Kelly, 1986 (16); Laursen, 1944
7	Igdlerussat	71.422	54.882	*New location*
8	Igdlerussat	71.422	54.882	*New location*
9	Tasiussaq	71.415	54.905	Bennike *et al*., 1994 (12)
10	Uligssat qôruat	71.436	54.031	*New location*

Table 2. Table of present chronological control from the southern and western Svartenhuk Peninsula. All ^{14}C except one returned infinite ages. Samples are from marine shells; *T. borealis, M. truncate, H. arctica, P. arctica and A. borealis.*

Log #	Elevation (m asl)	Age (^{14}C yrs BP)	$\delta^{13}C$‰	Reference
1	-	>40000	-	Kelly 1986
3	22	>40000	0.1	Bennike et al. 1994
5/6	7	>36600	-0.3	Bennike et al. 1994
11	0-2	37570±2570/1890	-	Bennike et al. 1994
12	8-10	>32530	1.4	Bennike et al. 1994
14	14	>30400	0.9	Bennike et al. 1994
16	35	>347100	0.2	Bennike et al. 1994

Table 3. Table of lithofacies associations, lithofacies, a short description of each lithofacies, and the facies/units from each logged section correlated to each lithofacies association.

Lithofacies		Sediment type	Units correlated to LFA
LFA1		Periglacially reworked bedrock	5a, 5b
LFA2		Lower matrix supported diamicton	1a, 2a, 5c, 6a, 9a
LFA3	**LFA3a**	Ice marginal glacio/fluviodeltaic bottomsets	7a, 8a, 9b-d, 10a
	LFA3b	Ice marginal glacio/fluviodeltaic foresets	1b, 2b, 3a, 4a, 7b-7d, 7f, 8b, 10b-e
	LFA3c	Ice marginal glacio/fluviodeltaic topsets	6b, 10f-g
LFA4		Slope deposits	3b, 9e
LFA5	**LFA5a**	Upper matrix supported diamicton	1c, 2c, 7e, 7g, 8c
	LFA5b	Esker gravel	7h, 8d

Table 4. Table of two new radiocarbon ages produced during this study, from Log 1, Arfertuarssuk. The results have been corrected to δ13CVPDB‰ -25 using the δ13C values seen above. Both samples from paired *Astarte montagui* bivalves. Calibrated ages were calculated using OxCal.

Code	Sample code	Lat. (°N)	Long (°W)	Sample type	$\delta^{13}C_{VPDB}$‰ ± 0.1	C content (% by wt.)	14C Enrichment (% modern)	+/- 1σ (% modern)	14C Age (years BP)	cal. Min (yr)	cal. Max (yr)	cal. mid (yr)
SUERC-37526	SV_1a (LFA2)	71.51	55.24	*Astarte montagui*	-0.265	11.5	0.41	0.06	44097 ±1177	*45604*	*49808*	*47706*
SUERC-37530	SV_1c (LF5a)	71.51	52.95	*Astarte montagui*	0.796	11.7	0.6	0.06	41106 ±810	*43552*	*46085*	*44819*

List of Figures

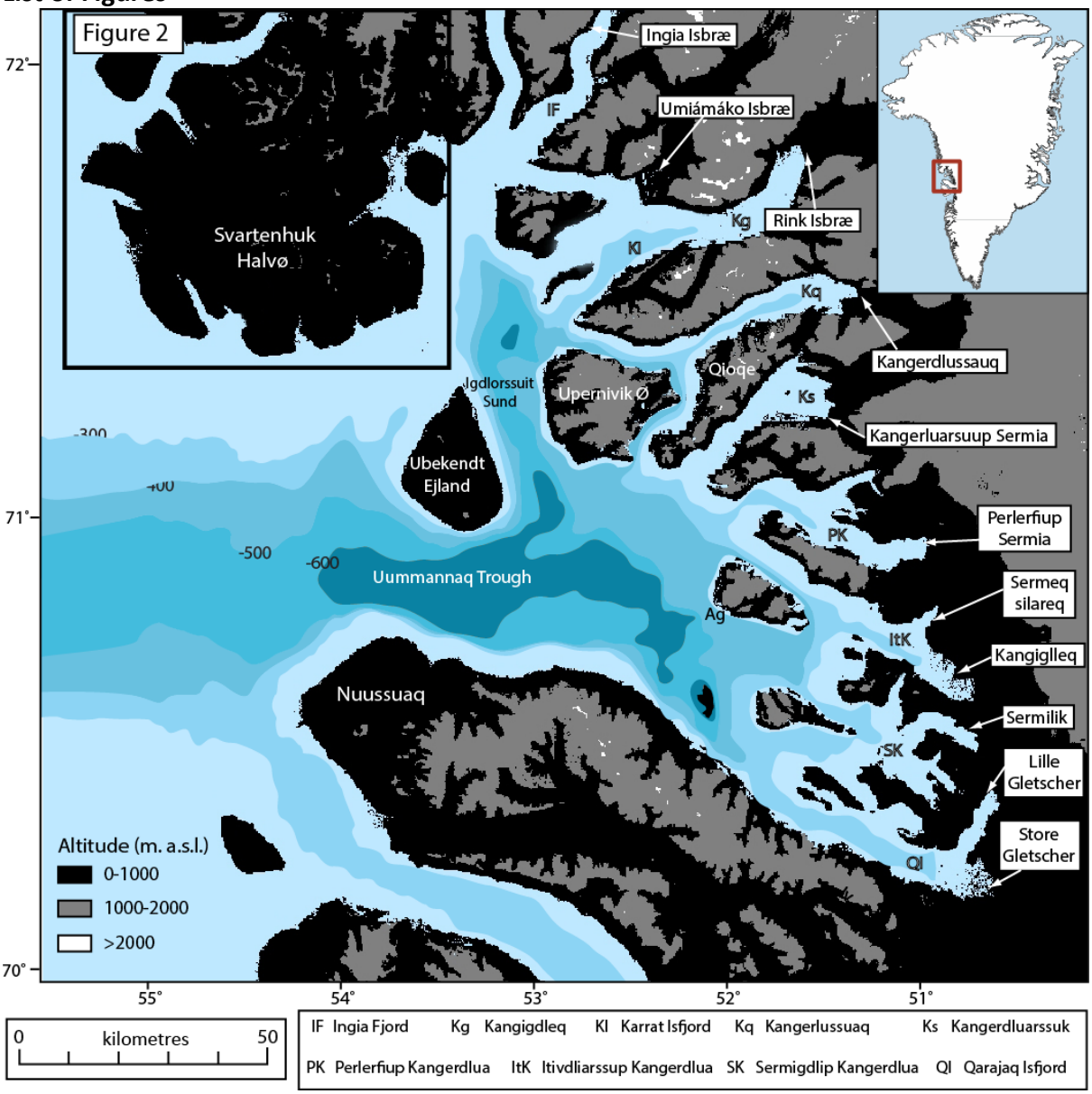

Figure 1. Topographic overview map of Uummannaq region. Altitudes are taken from ASTER imagery, and bathymetry from GEBCO.

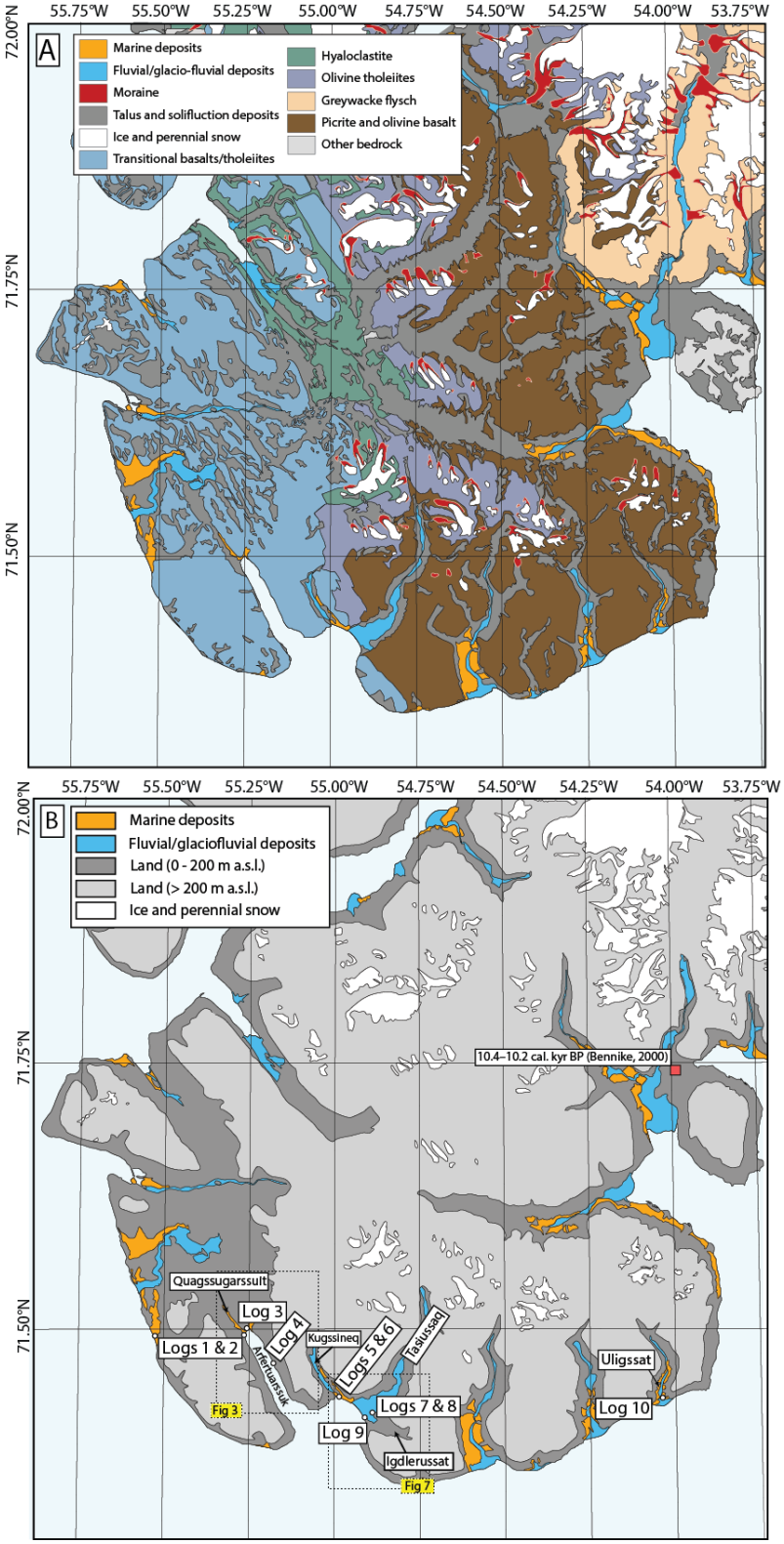

Figure 2. (A) Enlargement of the Svartenhuk Peninsula, with investigated sites and valleys discussed in the text labelled. In addition, surficial deposits of glaciofluvial/fluvial and marine sediment are shown, from Henderson and Pulvertaft (1987a,b). (B) Geology map of the Svartenhuk peninsula showing bedrock geology, and surficial deposits. Reproduced from (Henderson and Pulvertaft, 1987c). The calibrated radiocarbon age to the northeast of the region is from Bennike (2000), and represents the only Holocene shell age in the region.

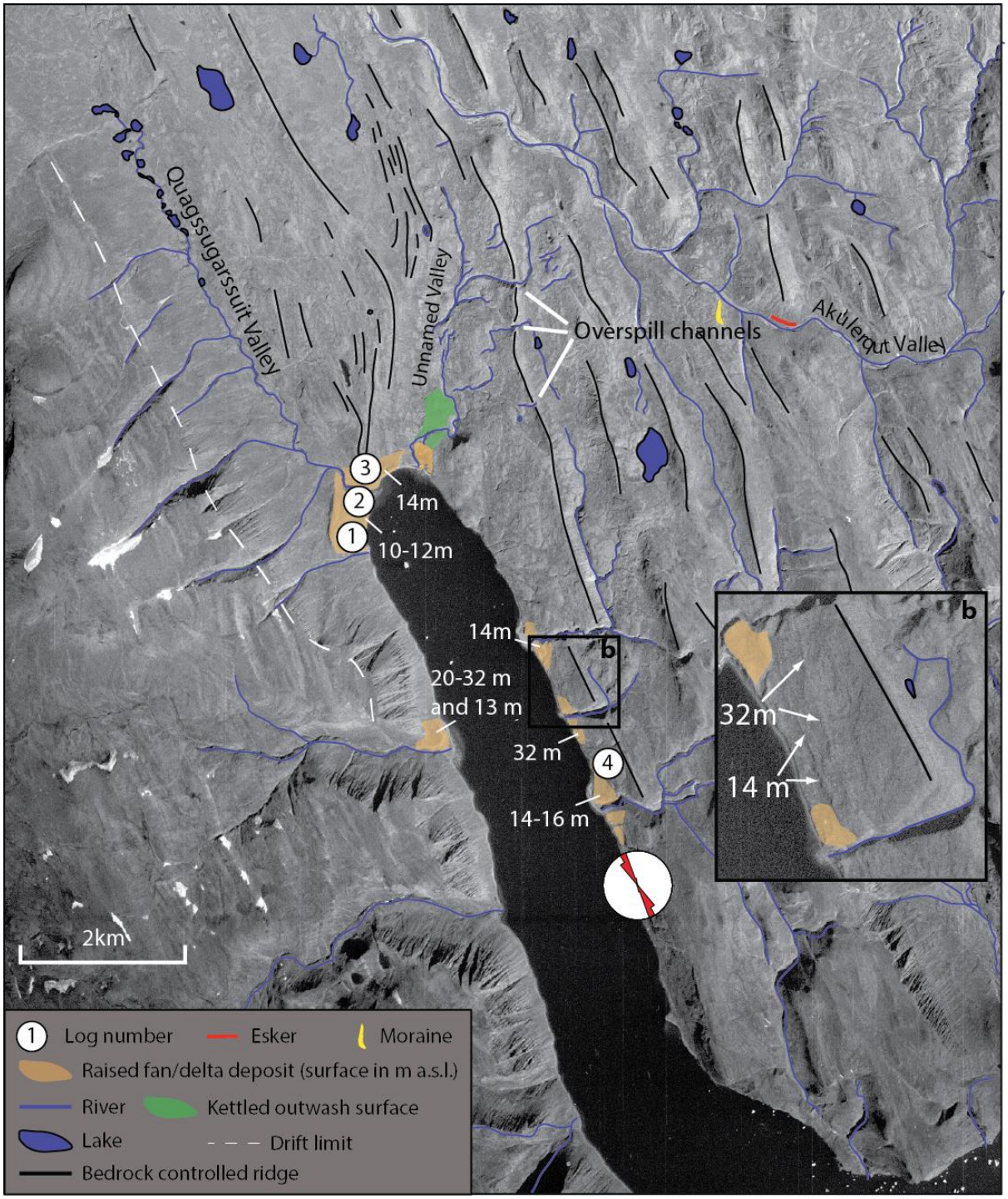

Figure 3. Geomorphological map of the Arfertuarssuk Fjord and Quagssugarssuit valley region, showing site numbers referred to in the text.

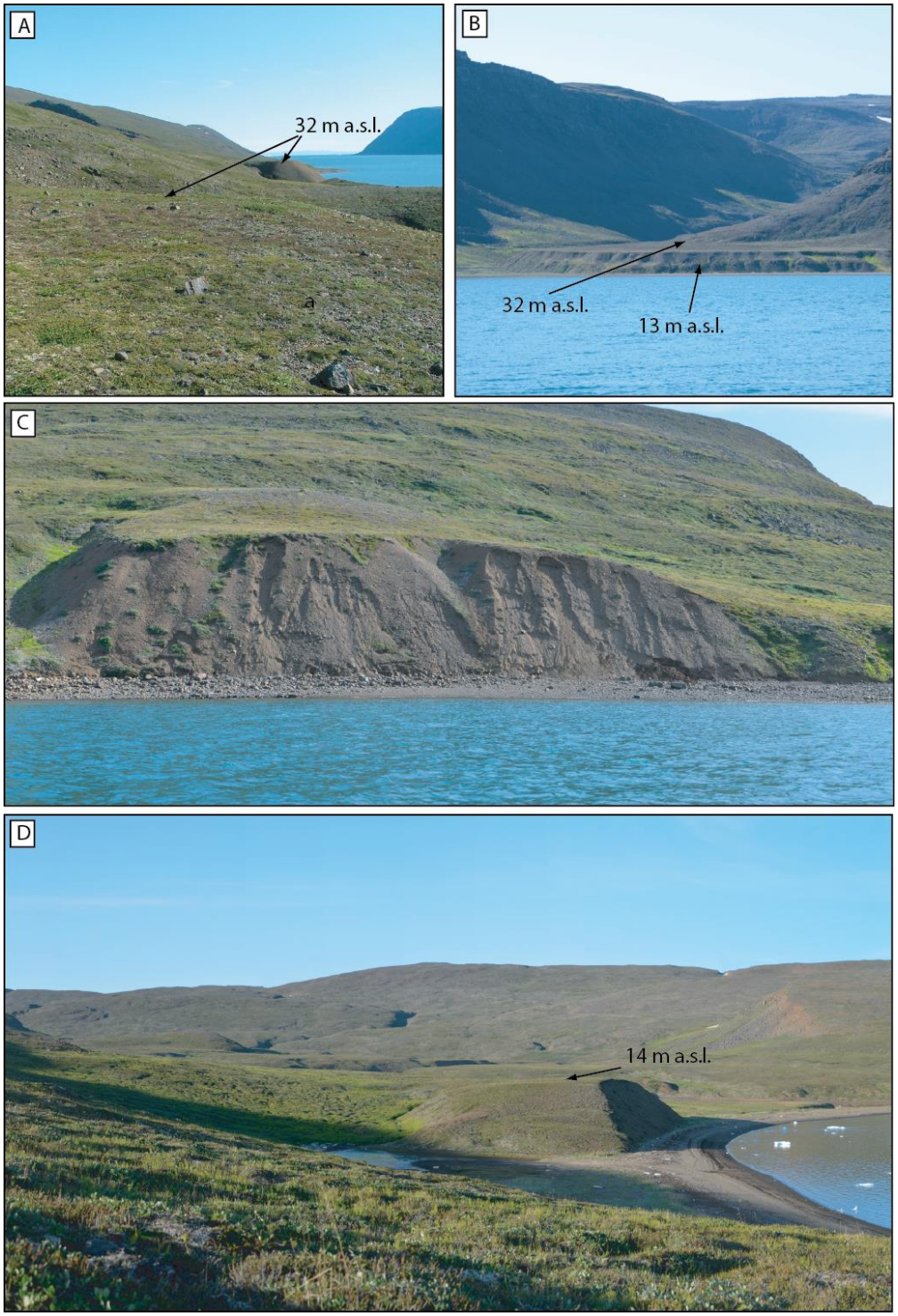

Figure 4. Photographs from Arfertuarssuk Fjord: (a) view south from the 32 m a.s.l. ridge north of Log 4 (see Figure 6.6) with clear alluvial fan graded to the same height; (b) view southwest from Log 4 to an extensive alluvial fan on the west side of the fjord. A clear dipping fan surface can be seen, with an incised step at 13 m a.s.l.; (c) view eastwards, looking directly at the location of Log 4 - bedding can be seen dipping toward the bottom right; (d) view from the surface of the sediment deposit from which Logs 1 and 2 were recorded, looking north east to the location of Log 3. Log 3 was recorded from the 14 m a.s.l. high mound in the centre of the photo. The valley in the background beyond this is the location in which extensive sediment and an esker were found (see text).

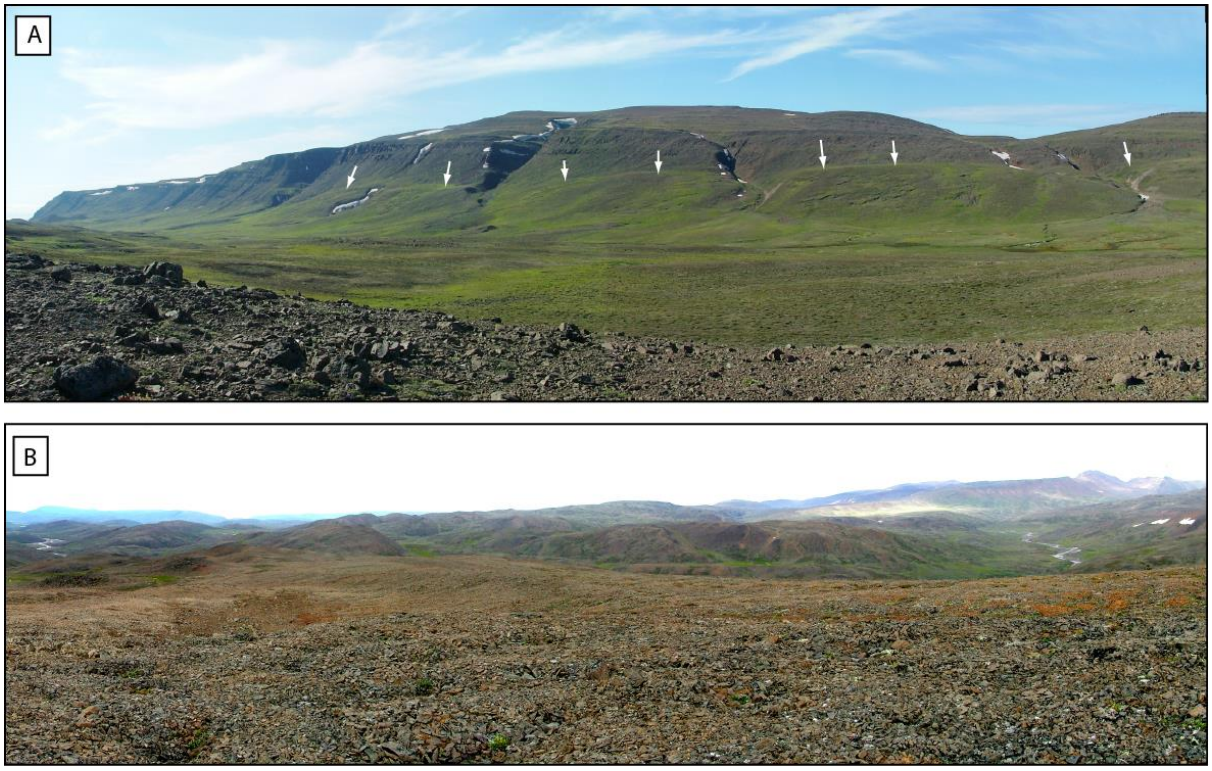

Figure 5. Photographs of the general morphology of the Quagssugarssuit region. (a) Photograph looking westward across the low-lying Quagssugarssuit valley. The higher ground in the background rises steeply to ~400 m a.s.l., and has distinct trimline/drift limit halfway up its face (arrowed). Arfertuarssuk fjord head is to the far left of the photograph; (b) heavily weathered and frost shattered terrain >300 m a.s.l., with a well-developed fluvial system in the lowlands to the left and right of the photograph.

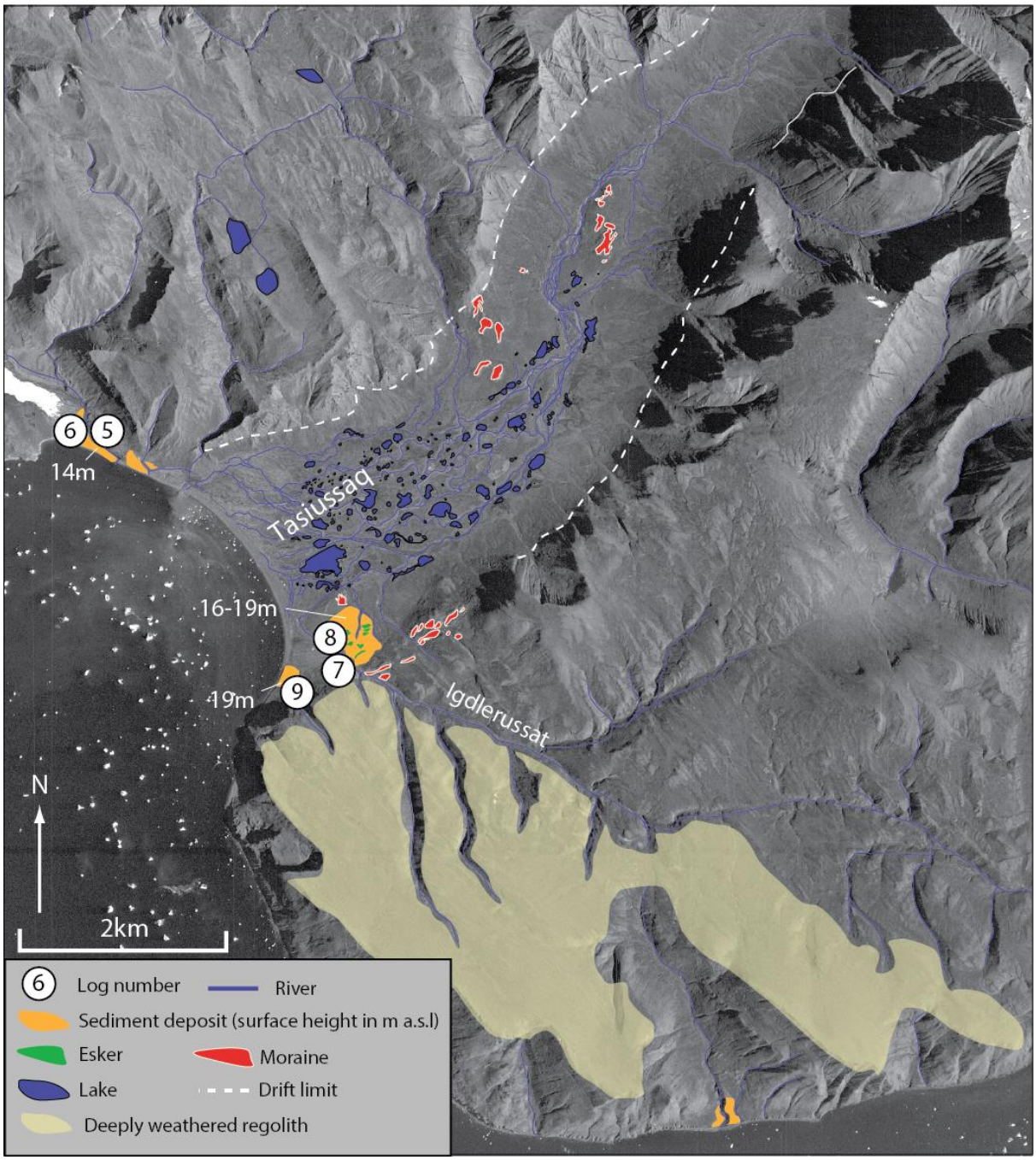

970
971 **Figure 6.** Geomorphological map of the Kugssineq valley and Tasiussaq region showing deposits and
972 landforms mapped during this study. Sites are labelled with numbers referred to in the text.
973

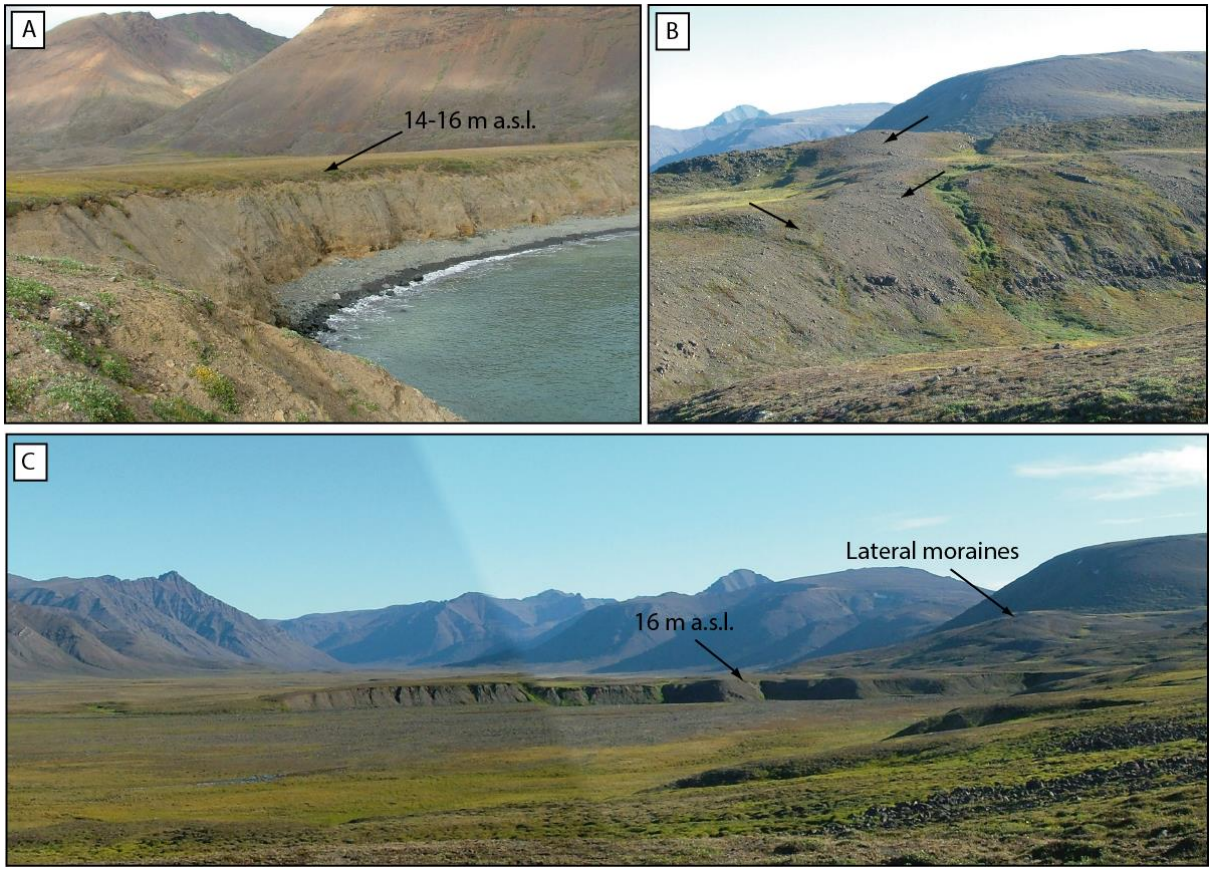

Figure 7. Photographs from the Kugssineq and Tasiussaq valleys. (a) view looking east at the cliff exposure of the delta at the mouth of the Kugssineq valley, the surface of which is graded to 14-16 m a.s.l. Logs 5 and 6 were taken from this exposure; (b) view looking northeast of the largest inset lateral moraines on the southern border of the Tasiussaq valley; (c) view of the Tasiussaq valley, looking northeast, up valley. The obvious flat topped feature in the centre is a delta, graded to 16 m a.s.l. Logs 7 and 8 were taken from the exposure facing the camera. In addition, inset lateral moraines can be seen to the right of the image.

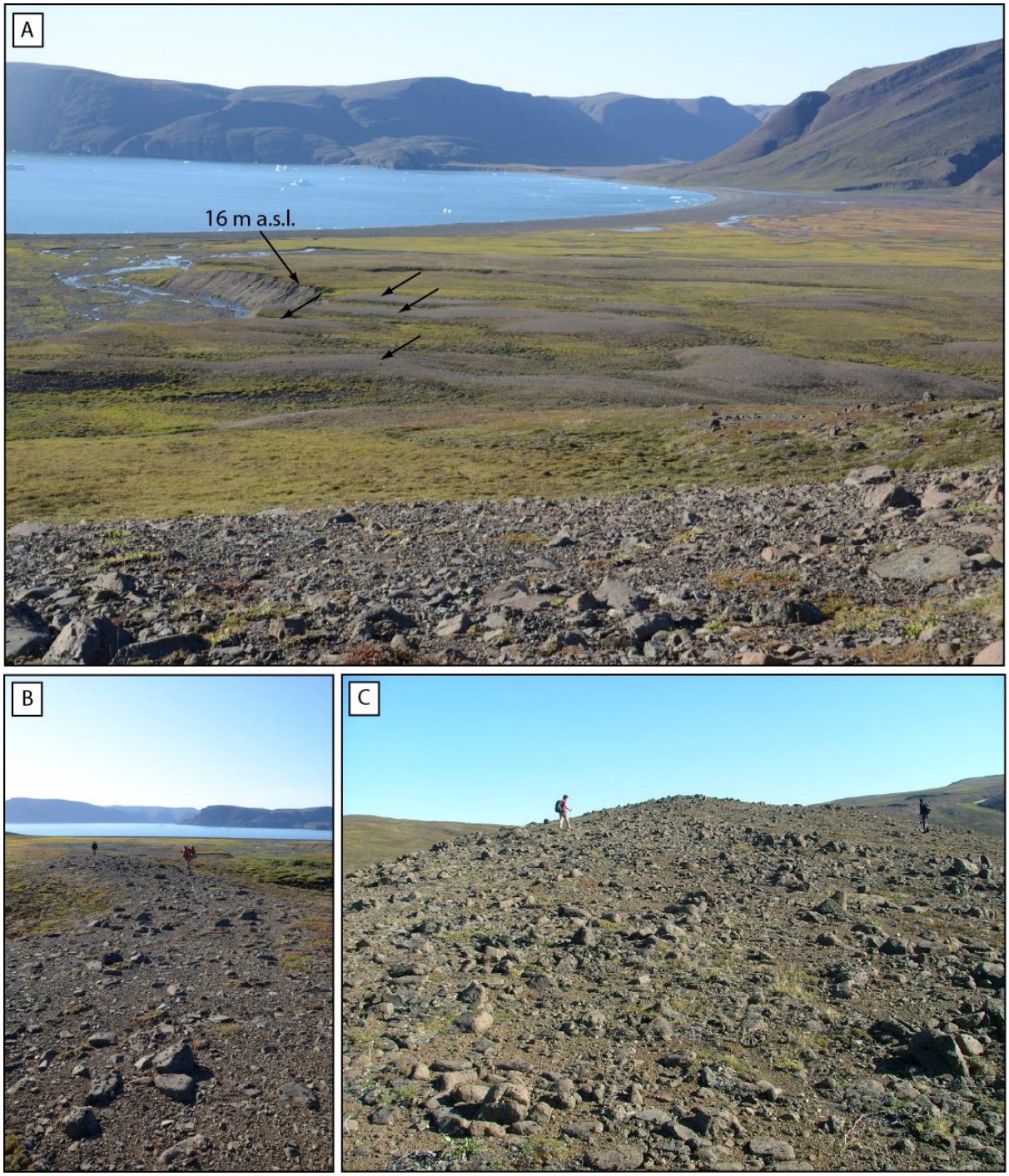

Figure 8. Photographs from Tasiussaq valley (a) oblique view looking northwest over the delta surface from which Logs 7 and 8 were recorded. Small sinuous graveliferous ridges are indicated by black arrows, trending from right to left across the photo. These are interpreted as eskers (see text for details); (b) view along a sinuous, low relief gravel esker overlying Site 7; (c) typical terrain outside the Tasiussaq lateral moraine limit - extensive heavily weathered regolith.

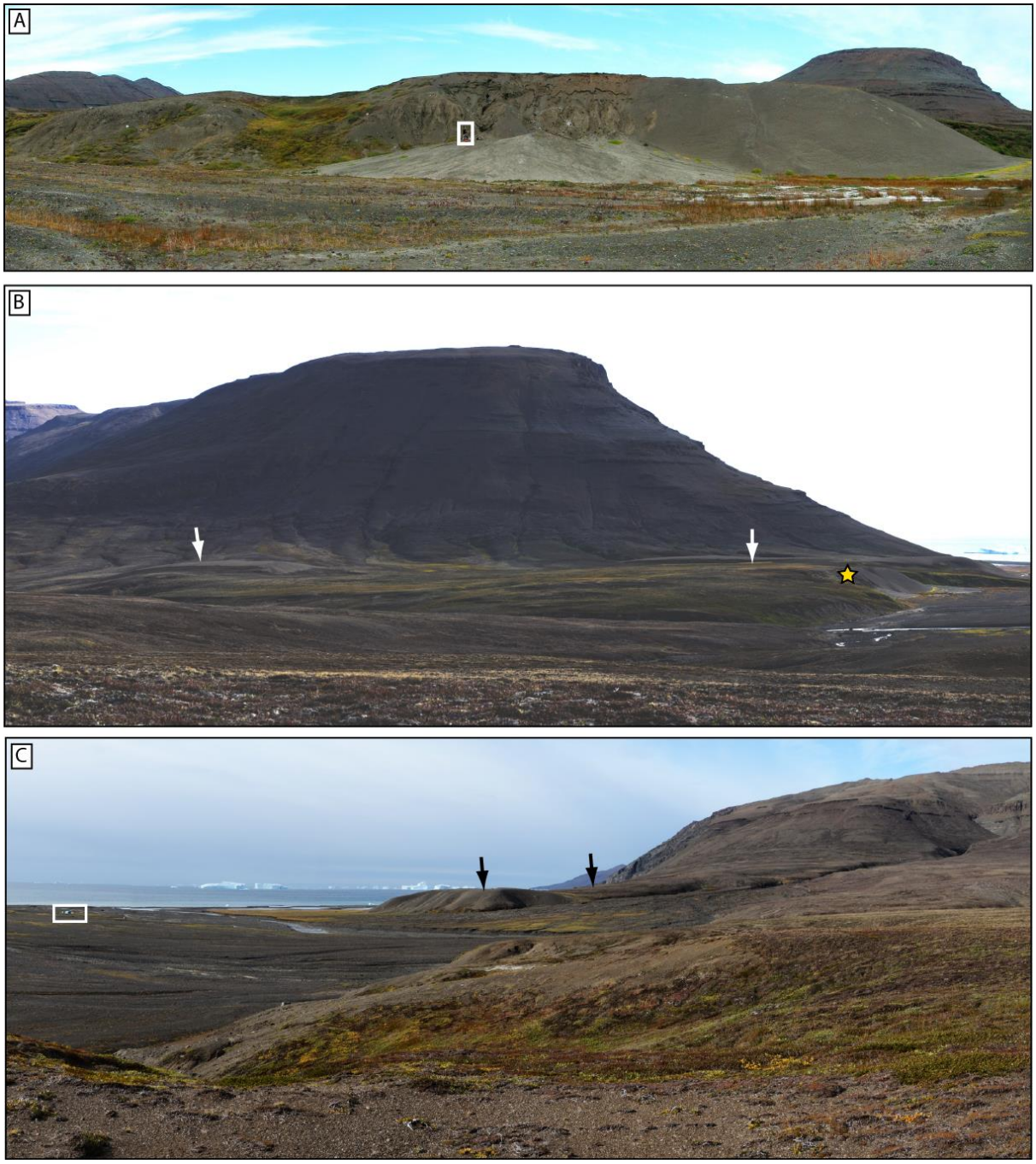

Figure 9. Plate of photographs from the Uligssat Valley (see Figure 6.3 for valley location). (a) photograph looking up-valley at the face of the delta, including the section logged in Log 10. A person can be seen surrounded by a box in the centre of the photograph for scale; (b) view looking east towards a raised delta (arrowed) in the mouth of the Uligssat valley. Location of Log 10 is shown by a star; (c) view westward from the delta surface seen in photograph C. A continuation of the logged delta surface is seen arrowed in the background. The area between the two surfaces is dissected by contemporary fluvial activity. Tents identified by a white box can be seen on the flat fluvial surface to the left for scale.

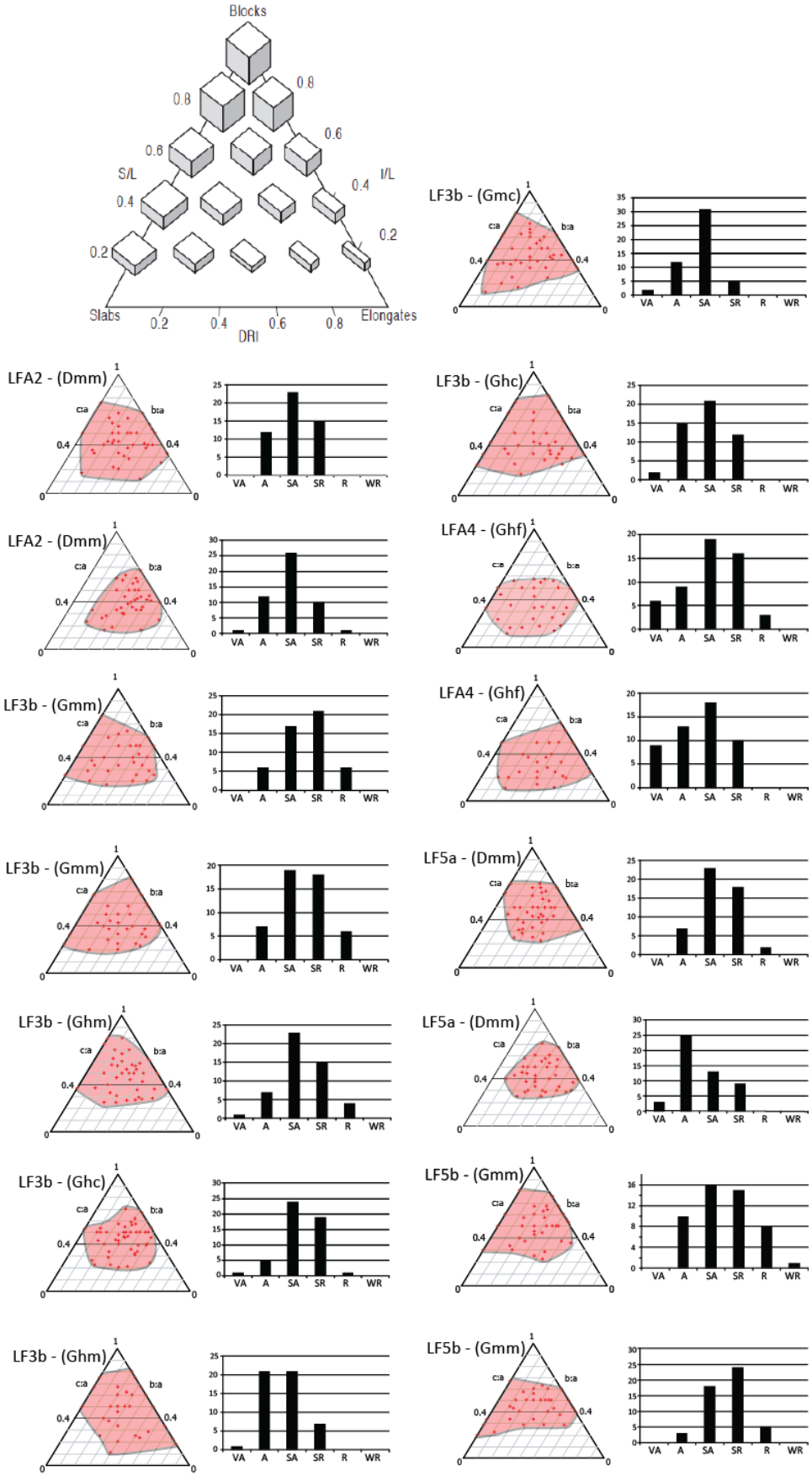

Figure 10. Clast form (triangle plots) and clast roundness (histograms) from a number of sites in the study. The specific facies of each sample location is marked, with the facies code.

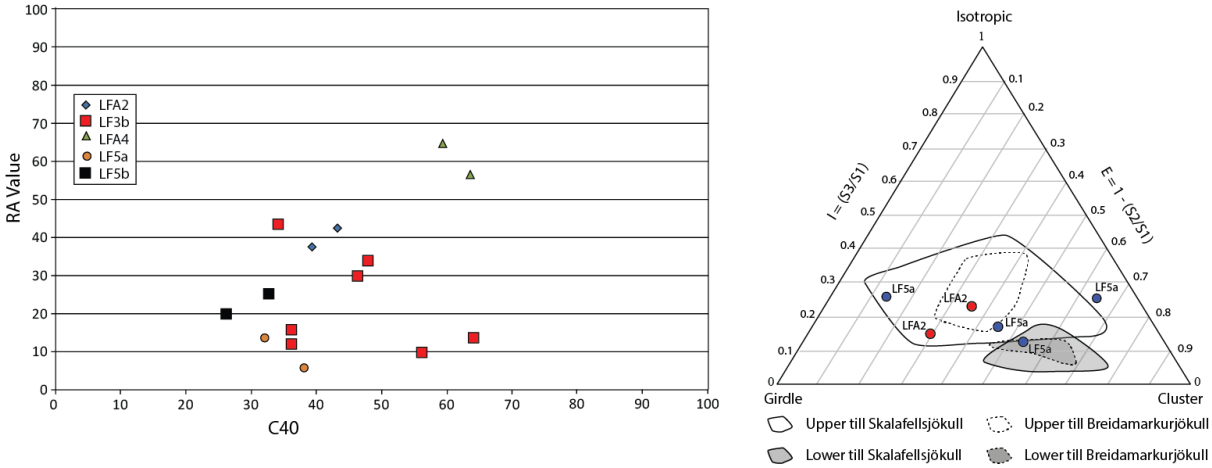

Figure 11. Plot of clast form data from this study, showing RA values against C40 values for all samples, with lithofacies codes labelled. Also, clast fabric triangle of samples from LFA2 and LF5a taken during this study (red circles), superimposed upon known fabric data from previous studies (Benn, 1994).

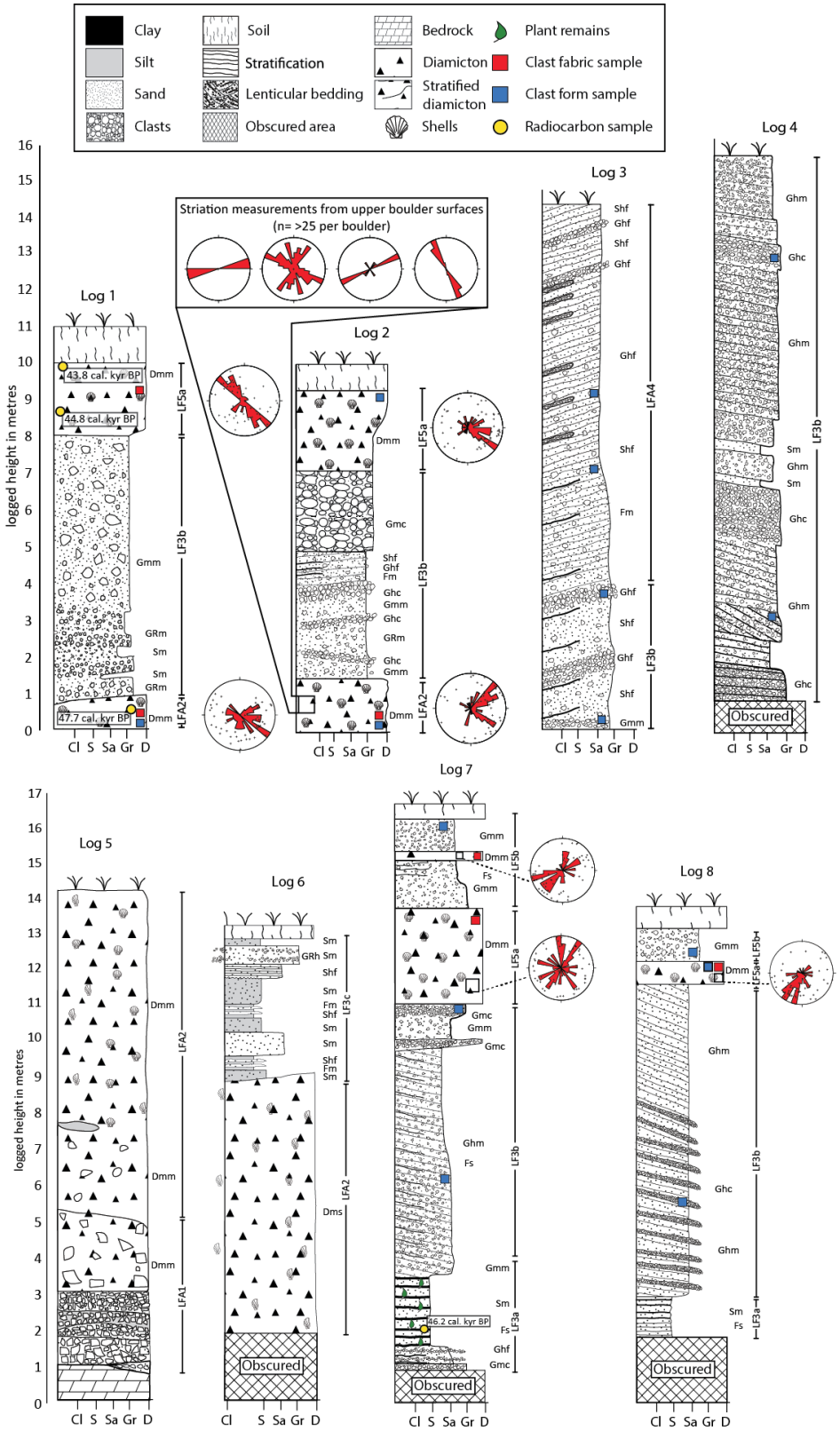

Figure 12. Sedimentary Logs 1-4, recorded from Arfertuarssuk Fjord, and Logs 5-8 from Tasiussaq Valley. Facies codes and sediment symbols outlined to the left are used throughout the chapter. Clast fabric directional data are shown in red stereonets. The inset box for Log 2 shows results of striae found on boulder from LFA2.

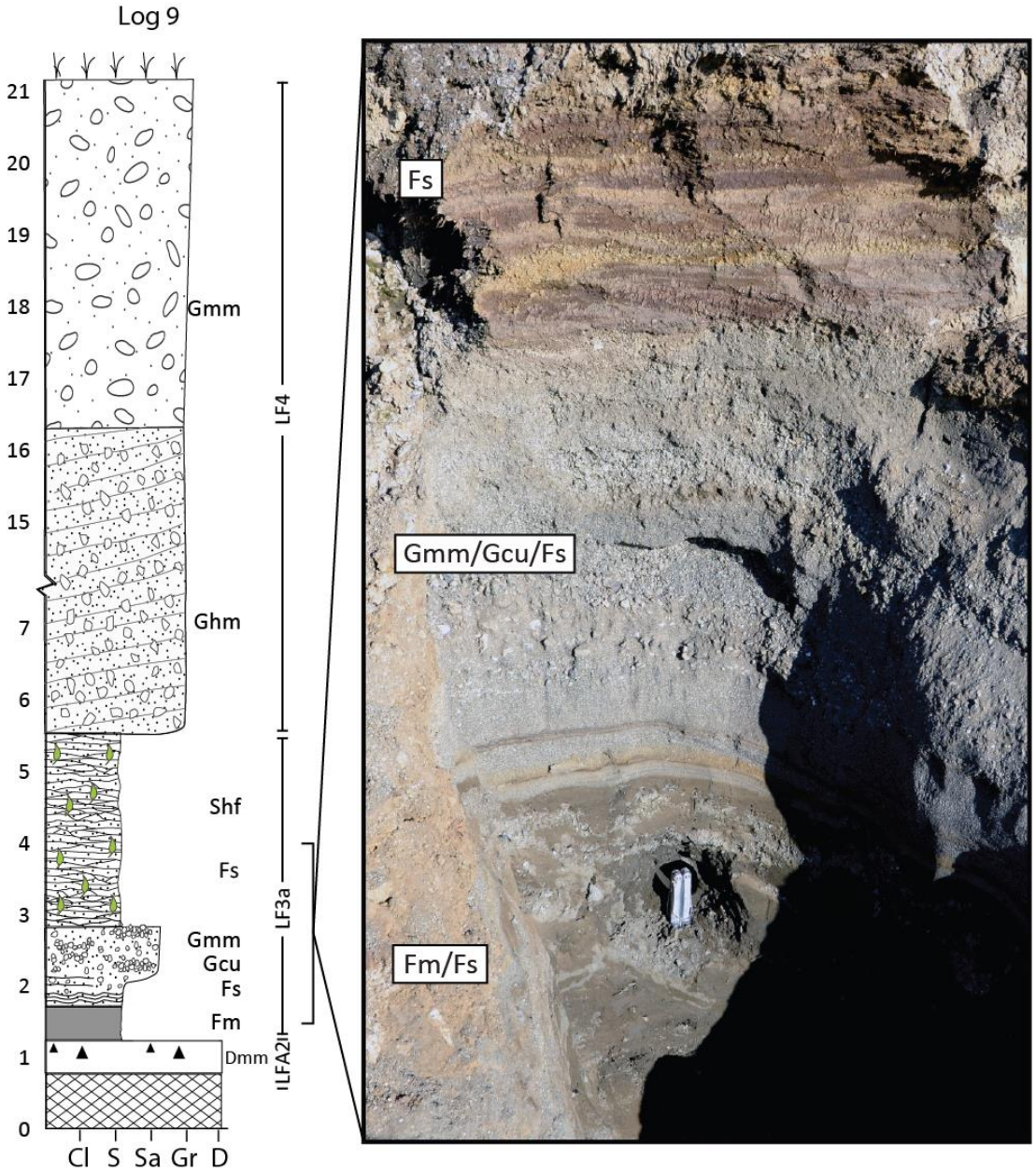

Figure 13. Log 9, from the mouth of Tasiussaq (see Figure 6.3 for location). Photograph to the right displays lithofacies 9b, 9c, and 9d, showing the difference in sedimentary properties between them. Note the extreme organic content of facies 9d in comparison to the minerogenic 9c.

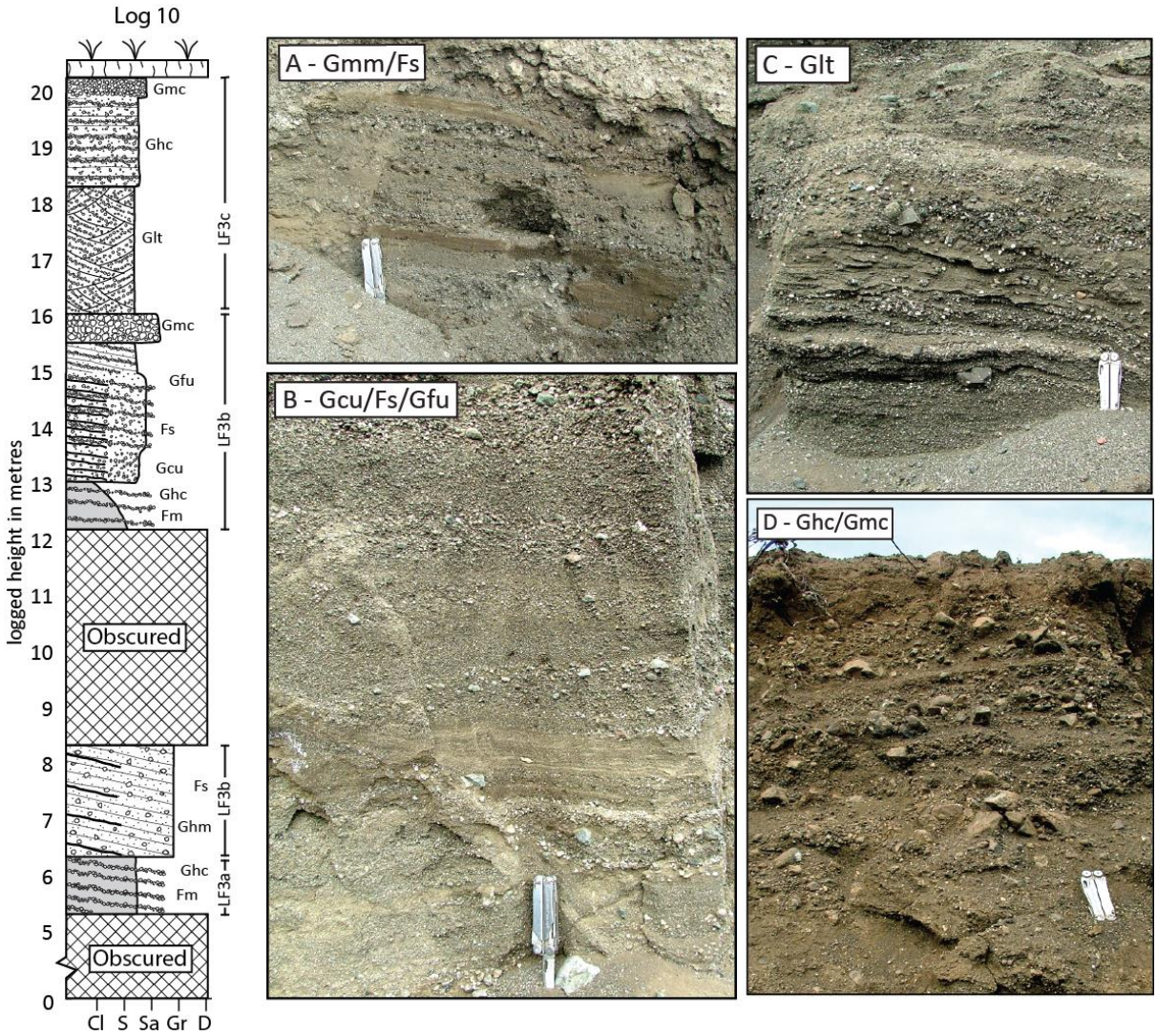

Figure 14. Sedimentary log and sediment photographs of Site 9, Log A. (a) dipping, interstratified silts, fine sands, and granules; (b) coarser deposits of sands and matrix supported gravels, still showing planar stratification; (c) coarser gravels, in places clast supported. Some planar stratification, some lenticular bedding; (d) horizontal, planar stratified gravels, with larger clasts than previous facies.

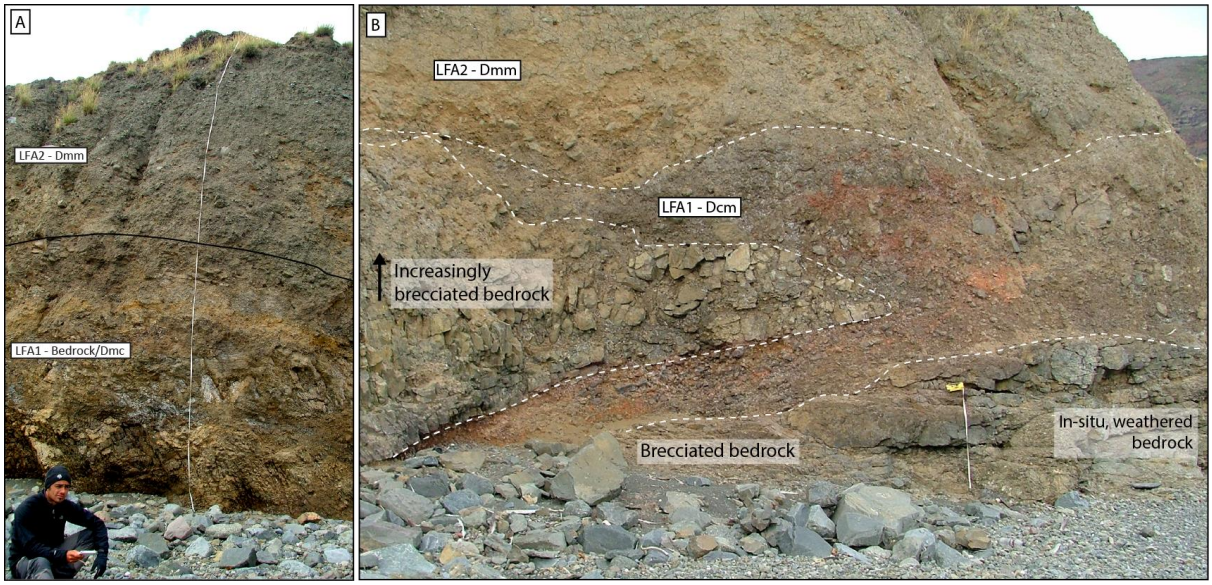

Figure 15. Photograph from Logs 5, showing the only exposure of LFA1. (a) overview of the section logged in Log 5; (b) enlargement of LFA1 and its contact with bedrock below, and LFA2 above. The interstratified/injected LFA1 can be seen. Tape measure is ~60 cm in length.

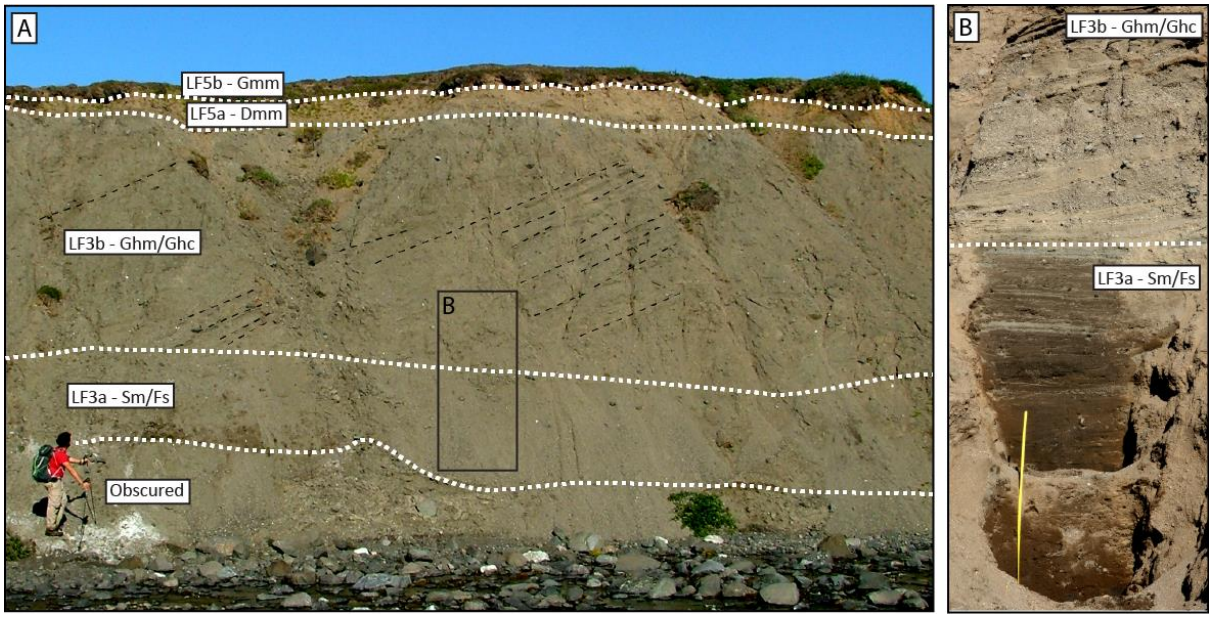

Figure 16. Photographs from the delta section recorded in Log 8. (a) overview photograph of the section described in Log 8, dominated by the dipping, planar stratified LF3b; (b) enlargement of facies 8a-b, showing the sharp switch from LF3a to LF3b.

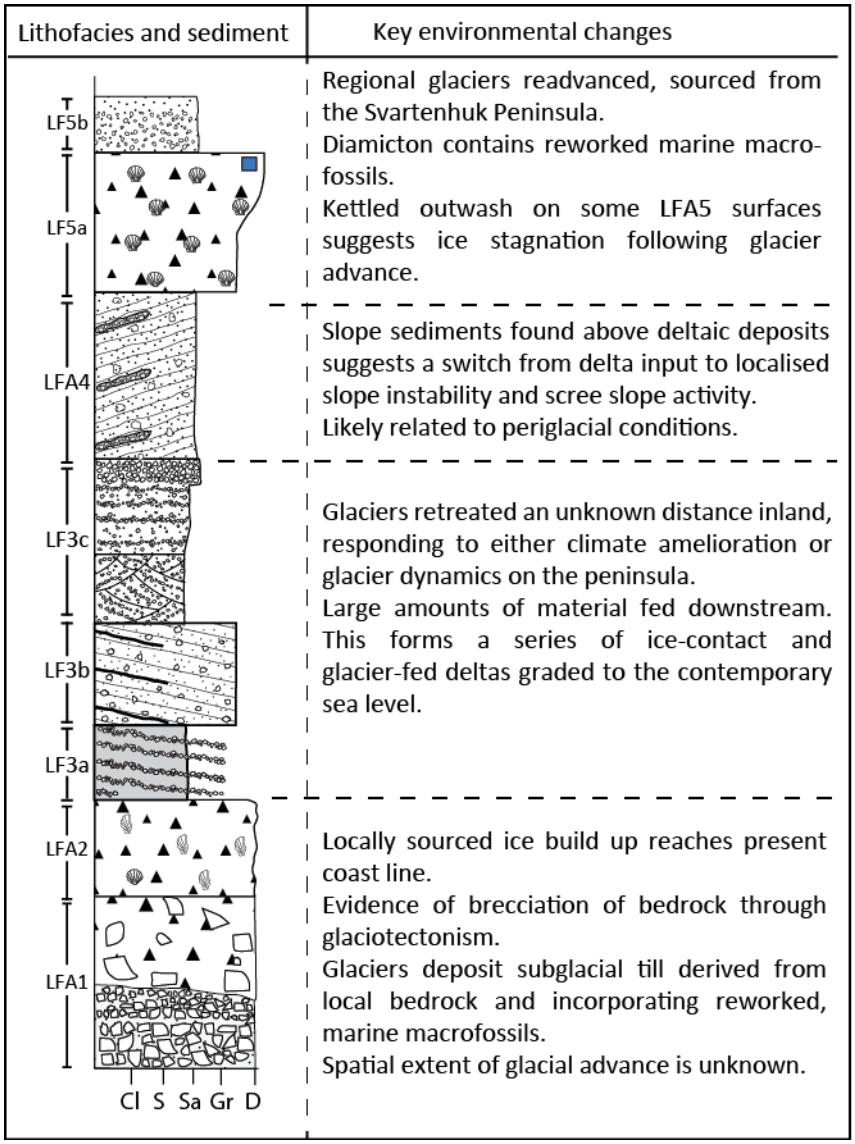

Figure 17. A composite sedimentary log from the study area.